



Slow Ca^{2+} Efflux by $\text{Ca}^{2+}/\text{H}^{+}$ Exchange in Cardiac Mitochondria Is Modulated by Ca^{2+} Re-uptake via MCU, Extra-Mitochondrial pH, and H^{+} Pumping by $\text{F}_0\text{F}_1\text{-ATPase}$

OPEN ACCESS

Edited by:

Miguel A. Aon,
National Institute on Aging (NIA),
United States

Reviewed by:

Karin Nowikovsky,
Medical University of Vienna, Austria
Elena N. Dedkova,
University of California, Davis,
United States

*Correspondence:

David F. Stowe
dfstowe@mcw.edu

† Present address:

Johan Haumann,
Department of Anesthesiology
and Pain Management, Maastricht
University Medical Centre, University
Pain Centre Maastricht, Maastricht,
Netherlands
Ashish K. Gadicherla,
Institute of Clinical Medicine,
University of Oslo, Oslo, Norway
Age D. Boelens,
Department of Anesthesiology,
Academic Medical Center, University
of Amsterdam, Amsterdam,
Netherlands
Christoph A. Blomeyer,
Department of Anesthesia and Critical
Care, University Hospital Würzburg,
Würzburg, Germany

Specialty section:

This article was submitted to
Mitochondrial Research,
a section of the journal
Frontiers in Physiology

Received: 16 July 2018

Accepted: 18 December 2018

Published: 04 February 2019

Johan Haumann^{1†}, Amadou K. S. Camara^{1,2,3,4}, Ashish K. Gadicherla^{1†},
Christopher D. Navarro¹, Age D. Boelens^{1†}, Christoph A. Blomeyer^{1†}, Ranjan K. Dash⁵,
Michael R. Boswell¹, Wai-Meng Kwok^{1,3,4,6} and David F. Stowe^{1,2,3,5,7*}

¹ Department of Anesthesiology, Medical College of Wisconsin, Milwaukee, WI, United States, ² Department of Physiology, Medical College of Wisconsin, Milwaukee, WI, United States, ³ Cardiovascular Center, Medical College of Wisconsin, Milwaukee, WI, United States, ⁴ Cancer Center, Medical College of Wisconsin, Milwaukee, WI, United States, ⁵ Department of Biomedical Engineering, Medical College of Wisconsin and Marquette University, Milwaukee, WI, United States, ⁶ Department of Pharmacology and Toxicology, Medical College of Wisconsin, Milwaukee, WI, United States, ⁷ Research Service, Veterans Affairs Medical Center, Milwaukee, WI, United States

Mitochondrial (m) Ca^{2+} influx is largely dependent on membrane potential ($\Delta\Psi_m$), whereas m Ca^{2+} efflux occurs primarily via Ca^{2+} ion exchangers. We probed the kinetics of $\text{Ca}^{2+}/\text{H}^{+}$ exchange (CHE_m) in guinea pig cardiac muscle mitochondria. We tested if net m Ca^{2+} flux is altered during a matrix inward H^{+} leak that is dependent on matrix H^{+} pumping by ATP_m hydrolysis at complex V ($\text{F}_0\text{F}_1\text{-ATPase}$). We measured $[\text{Ca}^{2+}]_m$, extra-mitochondrial (e) $[\text{Ca}^{2+}]_e$, $\Delta\Psi_m$, pH_m , pH_e , NADH, respiration, ADP/ATP ratios, and total $[\text{ATP}]_m$ in the presence or absence of protonophore dinitrophenol (DNP), mitochondrial uniporter (MCU) blocker Ru360, and complex V blocker oligomycin (OMN). We proposed that net slow influx/efflux of Ca^{2+} after adding DNP and CaCl_2 is dependent on whether the ΔpH_m gradient is/is not maintained by reciprocal outward H^{+} pumping by complex V. We found that adding CaCl_2 enhanced DNP-induced increases in respiration and decreases in $\Delta\Psi_m$ while $[\text{ATP}]_m$ decreased, ΔpH_m gradient was maintained, and $[\text{Ca}^{2+}]_m$ continued to increase slowly, indicating net m Ca^{2+} influx via MCU. In contrast, with complex V blocked by OMN, adding DNP and CaCl_2 caused larger declines in $\Delta\Psi_m$ as well as a slow fall in pH_m to near pH_e while $[\text{Ca}^{2+}]_m$ continued to decrease slowly, indicating net m Ca^{2+} efflux in exchange for H^{+} influx (CHE_m) until the ΔpH_m gradient was abolished. The kinetics of slow m Ca^{2+} efflux with slow H^{+} influx via CHE_m was also observed at pH_e 6.9 vs. 7.6 by the slow fall in pH_m until ΔpH_m was abolished; if Ca^{2+} reuptake via the MCU was also blocked, m Ca^{2+} efflux via CHE_m became more evident. Of the two components of the proton electrochemical gradient, our results indicate that CHE_m activity is driven largely by the ΔpH_m chemical gradient with H^{+} leak, while m Ca^{2+} entry via MCU depends largely on the charge gradient $\Delta\Psi_m$. A fall in $\Delta\Psi_m$ with excess m Ca^{2+} loading can occur during cardiac cell stress.

Cardiac cell injury due to mCa^{2+} overload may be reduced by temporarily inhibiting F_0F_1 -ATPase from pumping H^+ due to $\Delta\Psi_m$ depolarization. This action would prevent additional slow mCa^{2+} loading via MCU and permit activation of CHE_m to mediate efflux of mCa^{2+} .

HIGHLIGHTS

- We examined how slow mitochondrial (m) Ca^{2+} efflux via $\text{Ca}^{2+}/\text{H}^+$ exchange (CHE_m) is triggered by matrix acidity after a rapid increase in $[\text{Ca}^{2+}]_m$ by adding CaCl_2 in the presence of dinitrophenol (DNP) to permit H^+ influx, and oligomycin (OMN) to block H^+ pumping via F_0F_1 -ATP synthase/ase (complex V).
- Declines in $\Delta\Psi_m$ and pH_m after DNP and added CaCl_2 were larger when complex V was blocked.
- $[\text{Ca}^{2+}]_m$ slowly increased despite a fall in $\Delta\Psi_m$ but maintained pH_m when H^+ pumping by complex V was permitted.
- $[\text{Ca}^{2+}]_m$ slowly decreased and external $[\text{Ca}^{2+}]_e$ increased with declines in both $\Delta\Psi_m$ and pH_m when complex V was blocked.
- ATP_m hydrolysis supports a falling pH_m and redox state and promotes a slow increase in $[\text{Ca}^{2+}]_m$.
- After rapid Ca^{2+} influx due to a bolus of CaCl_2 , slow mCa^{2+} efflux by CHE_m occurs directly if pH_e is low.

Keywords: cardiac mitochondria, Ca^{2+} uptake/release, mitochondrial Ca^{2+} uniporter, $\text{Ca}^{2+}/\text{H}^+$ exchange, H^+ leak and pumping, complex V

INTRODUCTION

Mitochondrial (m) Ca^{2+} overload is a damaging consequence of cardiac ischemia-reperfusion (IR) injury and hence is an important subject for potential therapy (Brookes et al., 2004; O'Rourke et al., 2005; Stowe and Camara, 2009; Camara et al., 2010). During IR, mitochondria can consume rather than generate ATP (Chinopoulos and Adam-Vizi, 2010; Chinopoulos et al., 2010), which consequently can augment mCa^{2+} overload (Riess et al., 2002) sufficient to induce cell apoptosis and necrosis (Murphy and Steenbergen, 2008). $[\text{Ca}^{2+}]_m$ is regulated in part by electrochemical dependent cation flux via Ca^{2+} transporters and by cation exchangers within the inner mitochondrial membrane (IMM) (Gunter and Pfeiffer, 1990; Gunter et al., 1994; Bernardi, 1999; Brookes et al., 2004). The major route for mCa^{2+} uptake is via the ruthenium red (RR) sensitive mitochondrial Ca^{2+} uniporter (MCU), now considered a macromolecular complex composed of two pore components, MCU and MCU_b , and MCU regulators MCU_1 , 2, 3, and EMRE (essential MCU regulator), and other components (De Stefani et al., 2015). Ca^{2+} influx via the MCU is reduced by competition with cytosolic Mg^{2+} (Boelens et al., 2013; Tewari et al., 2014). Additional modes of mCa^{2+} uptake are proposed to occur via a ryanodine type channel (RTC) in the IMM (Ryu et al., 2011; O-Uchi et al., 2013; Tewari et al., 2014) and at the sarcoplasmic reticular-MCU interface where functional Ca^{2+} signaling between the cytoplasmic and mitochondrial compartments is believed to occur (Csordas et al., 2010).

A primary mCa^{2+} efflux pathway is the $\text{Na}^+/\text{Ca}^{2+}$ exchanger (NCE_m) (Boyman et al., 2013). In unicellular organisms and in some non-cardiac tissues there is firm evidence (Azzone et al., 1977; Pozzan et al., 1977; Wingrove et al., 1984; Brand, 1985; Rottenberg and Marbach, 1990; Gunter et al., 1991, 1994; Bernardi, 1999; Demaurex et al., 2009; Nishizawa et al., 2013) for slow homeostatic mCa^{2+} efflux through a Na^+ -independent Ca^{2+} exchanger (NICE), i.e., a non-electrogenic $\text{Ca}^{2+}/\text{H}^+$ exchanger (CHE) that might be activated when the ΔpH_m gradient across the IMM is altered. The amount of free (ionized) $[\text{Ca}^{2+}]_m$ available for exchange depends on the extent of dynamic mCa^{2+} buffering (Bazil et al., 2013; Blomeyer et al., 2013; Tewari et al., 2014). mCa^{2+} influx via the MCU and efflux via the NCE_m are largely voltage ($\Delta\Psi_m$) dependent, whereas Ca^{2+} transport via the CHE_m , while pH-dependent, may be electrogenic (1 H^+ for 1 Ca^{2+}) or non-electrogenic (2 H^+ for 1 Ca^{2+}). However, CHE_m can be indirectly dependent on the full IMM electrochemical gradient if there is a decrease in the IMM ΔpH_m gradient (Rottenberg and Marbach, 1990; Dash and Beard, 2008; Dash et al., 2009).

There is a well-known direct correlation between $\Delta\Psi_m$ and mCa^{2+} uptake based on the Nernst equation; a more polarized $\Delta\Psi_m$ permits greater mCa^{2+} uptake (Wingrove et al., 1984; Gunter et al., 1994). mCa^{2+} uptake via the MCU depends both on the electrical (charge) gradient, $\Delta\Psi_m$, and on the concentration gradient for $[\text{Ca}^{2+}]$ across the IMM. ATP_m hydrolysis with H^+ pumping can occur at complex V (F_0F_1 -ATP synthase/ase) during cardiac ischemia (Jennings et al., 1991) in an attempt to maintain the ΔpH_m gradient, and along with the $\Delta\Psi_m$

gradient (Chinopoulos and Adam-Vizi, 2010; Chinopoulos, 2011), equals the proton motive force, pmf . However, it is not known how the magnitude, rate, and route of mCa^{2+} uptake or release in cardiac muscle cell mitochondria is affected by manipulating the IMM $\Delta[\text{H}^+]_m$ gradient by allowing mATP hydrolysis, which would result in H^+ pumping and better maintain the $\Delta[\text{H}^+]_m$ gradient when $\Delta\Psi_m$ is low, vs. blocking mATP hydrolysis (no H^+ pumping with collapsing $\Delta[\text{H}^+]_m$) and lower $\Delta\Psi_m$.

Exposure of mitochondria to external (e) CaCl_2 when the IMM is fully charged (high $\Delta\Psi_m$), defined here by the presence of substrate in state 2 conditions without an induced inward H^+ leak, promotes rapid voltage-dependent mCa^{2+} uptake via MCU (Hoppe, 2010). In contrast, decreased net mCa^{2+} uptake might be expected during a protonophore-induced inward H^+ leak if H^+ influx leads to Ca^{2+} efflux. However, an inward H^+ flux that slowly decreases $\Delta\Psi_m$ can still result in a slow, continued uptake of mCa^{2+} via the MCU if there remains sufficient $\Delta\Psi_m$ and Ca^{2+} chemical gradient ($[\text{Ca}^{2+}]_e > [\text{Ca}^{2+}]_m$) across the IMM. mCa^{2+} influx via the MCU can partially depolarize $\Delta\Psi_m$ (Delcamp et al., 1998; Di Lisa and Bernardi, 1998) due to the influx of positive charges without an effect on the $\Delta[\text{H}^+]_m$, and more so with a fall in $\Delta[\text{H}^+]_m$ gradient from the added influx of H^+ in the presence of a protonophore.

Our aim was to mechanistically examine the slow mode kinetics of mCa^{2+} influx/efflux in cardiac cell mitochondria. The conditions under which CHE_m may occur in cardiac mitochondria are unknown. We proposed that an induced, net influx of H^+ is coupled to net mCa^{2+} efflux by activation of CHE_m in the face of continued mCa^{2+} uptake via the MCU in partially depolarized $\Delta\Psi_m$ mitochondria. In addition, if the extra-mitochondrial milieu is acidic, pH_m would slowly decrease as mH^+ entry by mCHE_m is exchanged for mCa^{2+} efflux in Ca^{2+} overloaded mitochondria. We postulated that CHE_m is activated under conditions of slow H^+ influx and a high $\text{m}[\text{Ca}^{2+}]_m$, and especially when H^+ pumping by complex V, stimulated by the lowered $\Delta\Psi_m$, is prevented. To carry out our aim, we examined the time dependent changes in $\Delta\Psi_m$, $[\text{Ca}^{2+}]_m$ and pH_m , and extra-mitochondrial $[\text{Ca}^{2+}]_e$ and pH_e , after a bolus of CaCl_2 either by inducing an inward H^+ leak that causes an outward pumping of H^+ by complex V, or by altering the extra-mitochondrial pH_e .

In one set of experiments, we challenged isolated energized mitochondria with a bolus of CaCl_2 in the absence or presence of increasing concentrations of the protonophore 2,4-dinitrophenol (DNP) in the absence or presence of the complex V inhibitor oligomycin (OMN) to block ATP hydrolysis-induced H^+ pumping, and or Ru360 to block the reuptake of Ca^{2+} via the MCU. To understand how DNP, OMN, and Ru360 dynamically alter $[\text{Ca}^{2+}]_m$ or $[\text{Ca}^{2+}]_e$ after a bolus of CaCl_2 , we considered it crucial to also dynamically measure $\Delta\Psi_m$, pH_m , and NADH, as well as mitochondrial respiration (extent of uncoupling), total $[\text{ATP}]_m$, and $\text{ATP}_m/\text{ADP}_m$ ratio. In another set of isolated mitochondrial experiments, we directly induced

mCa^{2+} efflux via CHE_m after CaCl_2 loading by altering the Na^+ -free medium from a control pH_e of 7.15 to either pH 7.6 or 6.9. We show that secondary Ca^{2+} influx vs. efflux is $\Delta[\text{H}^+]_m$ dependent.

MATERIALS AND METHODS

Isolated Mitochondrial Experiments

All experiments conformed to the Guide for the Care and Use of Laboratory Animal and were approved by the Medical College of Wisconsin Biomedical Resource Center animal studies committee. Detailed methods for mitochondrial isolation and measurements of $\Delta\Psi_m$, $[\text{Ca}^{2+}]_m$, NADH redox state, pH_m , $[\text{ATP}]_m$, $\text{ADP}_m/\text{ATP}_m$ ratio, respiration, and the number of animals per group, are furnished (see section “**Supplementary Materials S.1.1–S.1.12**”). Briefly, mitochondria were isolated from guinea pig heart ventricles in iced buffer and were suspended in experimental buffer containing in mM: KCl 130, K_2HPO_4 5, MOPS 20, bovine serum albumin 0.016 and EGTA $\sim 0.036\text{--}0.040$ at pH 7.15 (adjusted with KOH) at room temperature (21°C). The experimental buffer had a final protein concentration of 0.5 mg/mL. Specific fluorescent probes and spectrophotometry (Qm-8, Photon Technology International, Birmingham, NJ, United States) were used to measure $[\text{Ca}^{2+}]_m$ (indo-1AM) and buffer $[\text{Ca}^{2+}]_e$ (indo-1 or Fura 4 F penta- K^+ salt), NADH, an indicator of mitochondrial redox state (autofluorescence), pH_m (BCECF-AM), and mitochondrial membrane potential ($\Delta\Psi_m$) assessed by rodamine-123 or TMRM (Heinen et al., 2007; Huang et al., 2007; Aldakkak et al., 2010; Haumann et al., 2010) (all fluorescence probes from InvitrogenTM – Thermo Fisher Scientific). Respiration (Clark electrode) and ATP_m (bioluminescence) and $\text{ATP}_m/\text{ADP}_m$ ratio (HPLC, luminometry) were also measured. The experimental buffer, mitochondrial substrates, and drugs were Na^+ -free to prevent activation of NCE_m by extra-mitochondrial Na^+ . The inactivity of the NCE was verified by comparing data from these experiments to data from experiments with added CGP-37157, a known mitochondrial NCE_m inhibitor (data not shown).

Experimental Protocols

Medium pH_e -Induced Changes in pH_m

The experimental buffer was identical to that described above except that in addition to the pH 7.15 buffer, buffers at pH 6.9 and 7.6 were prepared by titration with HCl and KOH, respectively. The residual EGTA carried over from the isolation buffer to the experimental buffer resulted in an ionized extra-mitochondrial $[\text{Ca}^{2+}]_e$ of <200 nM (Figure 1). To measure changes in $[\text{Ca}^{2+}]_e$ after adding a bolus of 40 μM CaCl_2 , each pH buffer contained Fura 4 F penta- K^+ salt. The K_D 's for Ca^{2+} were calculated and corrected for each buffer pH because pH affects the binding of Ca^{2+} to the fluorescence dye (see section “**Supplementary Materials S.1.4, S.1.8**”). In other experiments, pH_m and $\Delta\Psi_m$ were measured using BCECF-AM and TMRM fluorescent dyes, respectively. Experiments were initiated at $t = 30$ s when mitochondria were added to the

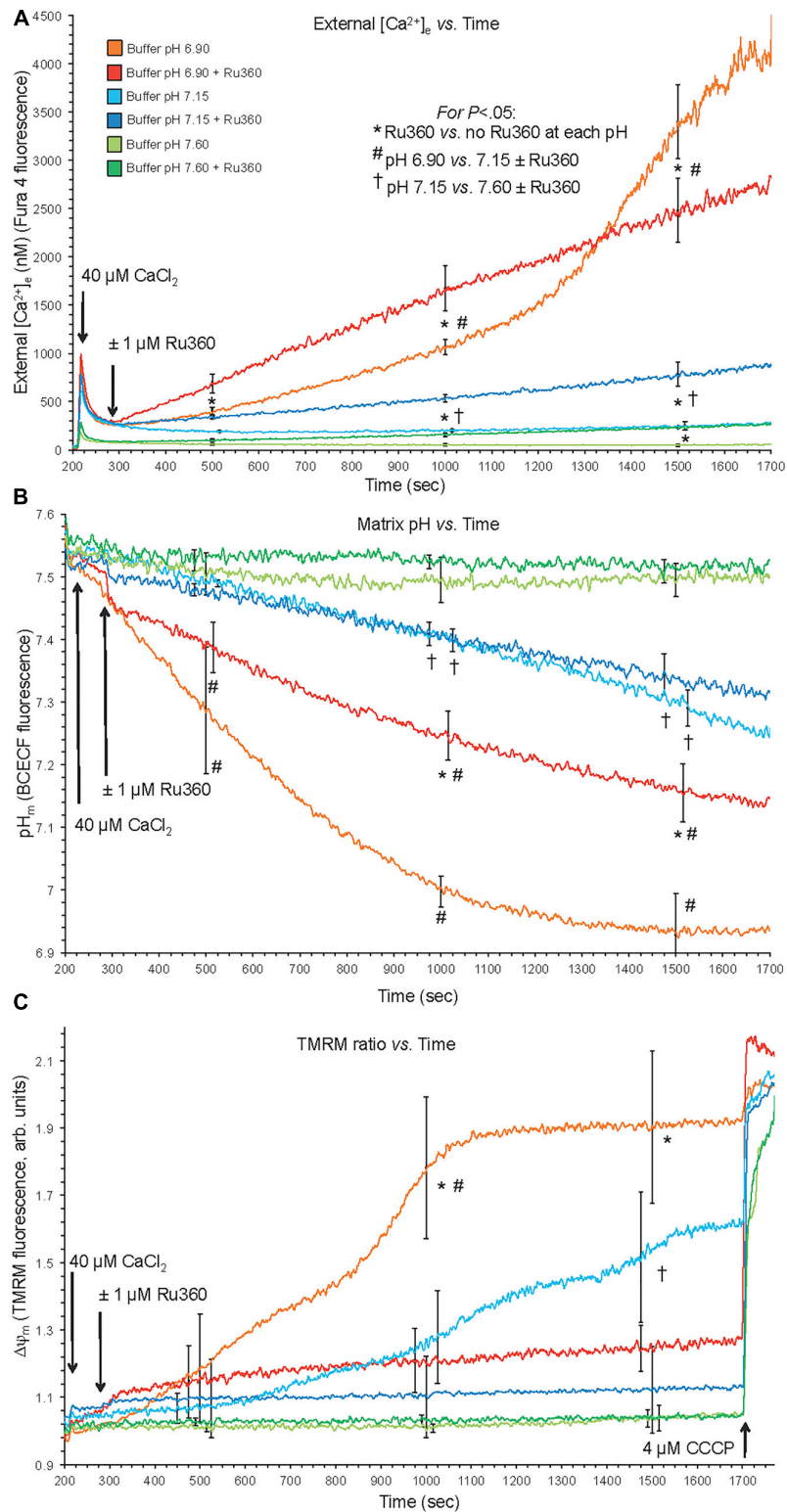
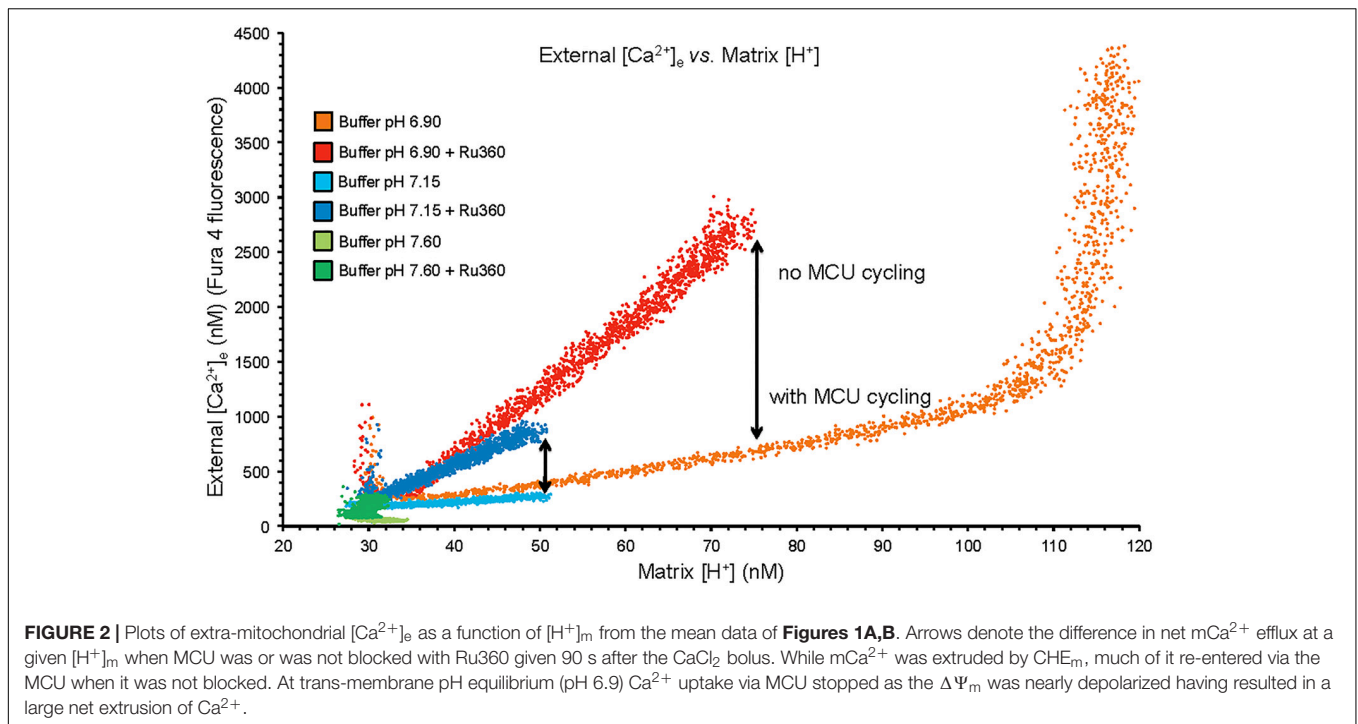


FIGURE 1 | Changes in buffer $[\text{Ca}^{2+}]_e$ (A), matrix pH_m (B), and $\Delta\Psi_m$ (C) over time after adding 40 μM CaCl_2 (210 s) at extra-mitochondrial pH_e 7.6, 7.15, and 6.9 with or without 1 μM Ru360 (300 s) to inhibit additional mCa^{2+} uptake via MCU. Note the rapid fall in $[\text{Ca}^{2+}]_e$ due to fast mCa^{2+} uptake via the MCU and the following slow rise in $[\text{Ca}^{2+}]_e$ (Ca^{2+} efflux) (A), slow decline in pH_m (B), and slow depolarization of $\Delta\Psi_m$ (C) at pH 6.9 (each line = mean of 3–4 replicates from 12 guinea pig hearts for each fluorescence measurement). Note in the pH 6.9 medium the faster rate of mCa^{2+} efflux (A) over time when MCU was blocked, and the faster declines in pH_m (B) and $\Delta\Psi_m$ (C) over time when MCU was not blocked.

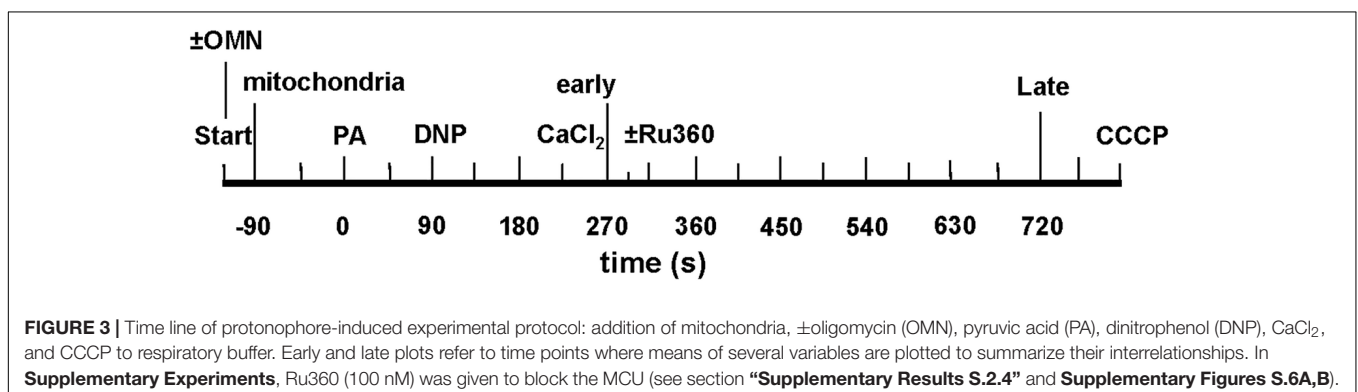


buffer; at $t = 90$ s pyruvic acid (PA, 0.5 mM) was added, followed by a bolus of 40 μM CaCl_2 at $t = 210$ s to initiate rapid mCa^{2+} uptake via MCU. Note that in guinea pig cardiac mitochondria, the respiratory control index (RCI) is higher in the presence of pyruvate alone (Heinen et al., 2007; Blomeyer et al., 2013; Boelens et al., 2013) than with pyruvate plus malate (Riess et al., 2008). For some experiments, 1 μM Ru360 (or vehicle, 0.1% DMSO) was added at $t = 300$ s shortly after adding CaCl_2 to block Ca^{2+} reuptake into mitochondria via MCU after the Ca^{2+} was extruded from mitochondria. At the end (1700 s) of each experiment, the potent protonophore, carbonyl cyanide m-chlorophenyl hydrazone (CCCP, 4 μM) was given to completely abolish the ΔpH gradient and depolarize $\Delta\Psi_m$. Data for each pH group were collected in mitochondrial suspensions from the same heart; approximately 8–10 hearts were used for each fluorescent probe. At pH 7.15, adding 40 μM CaCl_2 , which increased extra-mitochondrial $[\text{Ca}^{2+}]_e$ into the

1 μM range and increased the initial $[\text{Ca}^{2+}]_m$ to approximately 500 nM (**Figures 1, 2**), is unlikely to induce membrane permeability transition pore (mPTP) opening. However, to test the possibility of mPTP opening, 500 nM cyclosporine A (CsA), a modulator of cyclophilin D required to open mPTP, was given before adding CaCl_2 in several experiments at pH_e 6.9 and 7.15.

Protonophore-Induced Changes in pH_m

Experiments were initiated at $t = -120$ s; at $t = -90$ s, mitochondria were added to the experimental buffer (time line, **Figure 3**); external pH_e was 7.15. At $t = 0$ s, pyruvic acid (PA, 0.5 mM) was added to the mitochondria suspended in the experimental buffer, followed by 0, 10, 20, 30, or 100 μM DNP, a mild protonophore, at $t = 90$ s, followed by the addition of de-ionized H_2O , 10, or 25 μM CaCl_2 at $t = 225$ s. The 90 s period allowed for full $\Delta\Psi_m$ polarization



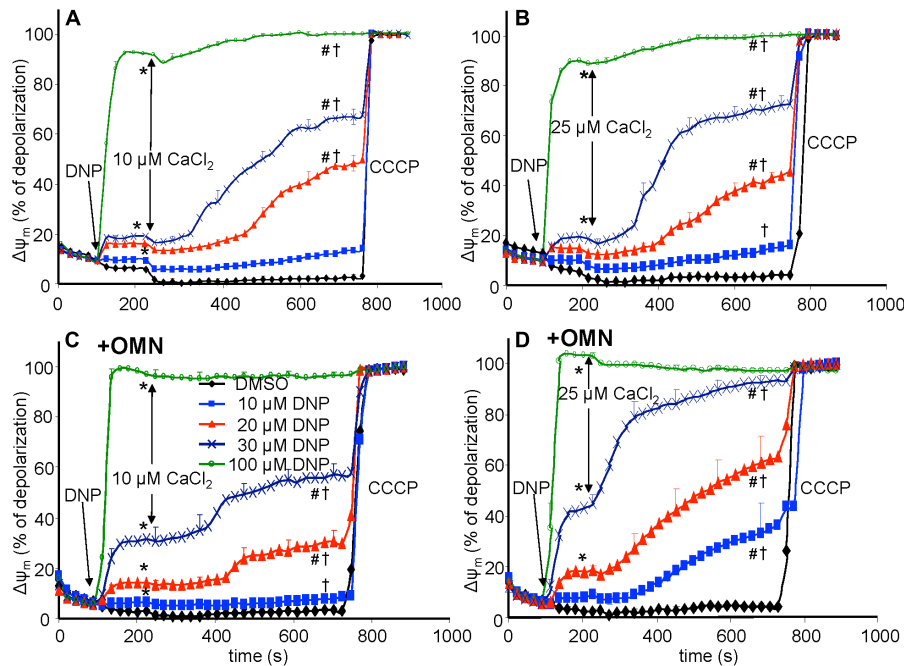


FIGURE 4 | Change in mitochondrial membrane potential ($\Delta\Psi_m$), assessed with rhodamine-123 as % of maximal depolarization, as a function of time after adding dinitrophenol (DNP) and CaCl_2 in the absence (A,B) and presence (C,D) of oligomycin (OMN). Note that adding DNP caused a concentration-dependent fall in $\Delta\Psi_m$ that was more pronounced in the presence of OMN. Adding CaCl_2 caused a small polarization, while increasing depolarization occurred over time. Adding 25 μM CaCl_2 (B,D) resulted in a more pronounced fall in $\Delta\Psi_m$ compared to 10 μM CaCl_2 (A,C). Buffer pH = 7.15. Data obtained from 10 hearts with 4–5 replicates per heart. For $P < 0.05$: *after DNP vs. before DNP; #after CaCl_2 vs. before CaCl_2 ; †late (700 s) vs. early (215 s) after CaCl_2 .

and stabilization of pH_m and NADH. In some experiments (see section “Supplementary Results S.2.4” and Supplementary Figure S.6), 100 nM Ru360 was added at $t = 300$ s, after the addition of CaCl_2 , to block any reuptake of mCa^{2+} by the MCU that was extruded by CHE_m . For the OMN treated groups, 10 μM OMN was added to the experimental buffer at the start of the experimental protocol (Figure 3). At the end of each experiment CCCP was added at $t = 760$ s to maximally depolarize $\Delta\Psi_m$. DNP, Ru360, OMN, and CCCP were each dissolved initially in DMSO and then in buffer to yield a final buffer concentration for DMSO of 0.1 to 0.4% (wt/vol). Each drug or DMSO alone was added to a final volume of 10 μL . To test for mPTP opening, CsA was given before adding 20 or 30 μM DNP and 25 μM CaCl_2 in several experiments conducted at pH_e 7.15.

Statistical Analyses

Data were summarized at 500, 1000, and 1500 s (for Figures 1, 2) for external buffer-induced changes in pH_m on $[\text{Ca}^{2+}]_e$. Data were summarized for protonophore-induced changes in pH_m on $[\text{Ca}^{2+}]_m$ at 80 s (after adding PA), 215 s (after adding DNP), 275 s (early after adding CaCl_2), and 700 s (late after adding CaCl_2) (e.g., Figure 4). All data points were presented and expressed as average \pm SEM. Repeated measure ANOVAs followed by a *post hoc* analyses using Student-Newman-Keuls’ test was performed to determine statistically significant differences among groups. A P -value < 0.05 (two-tailed)

was considered significant. See Figure legends for statistical notations.

RESULTS

CHE_m Activation Was Exposed by Efflux of Ca^{2+} With Influx of H^+ and Was Greater If MCU Was Inhibited

Direct evidence for CHE_m activation was observed by acidifying the extra-mitochondrial buffer (low pH_e), which subsequently decreased the matrix pH_m slowly over time (Figure 1). With NCE_m and Na^+/H^+ (NHE_m) inactivated by using Na^+ -free solutions and substrates, fast mCa^{2+} influx via the MCU, induced after adding 40 μM CaCl_2 at pH 6.9, was followed by a slow mCa^{2+} efflux over time $\sim(300\text{--}1700$ s) as shown by the increase in extra-mitochondrial $[\text{Ca}^{2+}]_e$ from <200 nM to nearly 4500 nM in the absence of Ru360 (Figure 1A). When Ru360 was added 90 s after adding CaCl_2 , $[\text{Ca}^{2+}]_e$ rose even more over the first 1000 s, indicating blockade of Ca^{2+} recycling via the MCU and revealing the total mCa^{2+} effluxed via CHE_m . In the pH 6.9 plus Ru360 group the mean rate (slope) of increase in $[\text{Ca}^{2+}]_e$ (mCa^{2+} efflux) over time (300–1700 s) was 1.5 ± 0.1 nM/s, ΔpH 0.4 units). This was greater than in the pH 6.9 minus Ru360 group (1.0 ± 0.2 nM/s over 300–1000 s), suggesting that approximately 1/3 of the mCa^{2+} extruded was retaken up across the IMM

via the MCU. In contrast, mCa^{2+} efflux was not observed in the pH 7.6 medium without Ru360, and minimally at 1500 s at pH 7.6 with Ru360. There was less mCa^{2+} efflux at pH $7.15 \pm \text{Ru360}$ compared to pH $6.9 \pm \text{Ru360}$. However, even at pH $7.15 \pm \text{Ru360}$, there were similar steady declines in pH_e while net slow Ca^{2+} efflux was noted only in the plus Ru360 groups, indicating Ca^{2+} re-uptake via MCU. Therefore, in the acidic extra-mitochondrial medium, slow decreases in pH_m (H^+ influx) were accompanied by slow increases in mCa^{2+} efflux, indicating CHE_m activity. Eventually, matrix acidification was more pronounced in the pH 6.9 medium (ΔpH 0.62 units) in the absence of Ru360 than in all other groups so that over time as H^+ influx was exchanged for Ca^{2+} efflux the IMM ΔpH gradient was eventually obliterated, halting Ca^{2+} efflux (Figure 1B). Eventually, because of mCa^{2+} influx, near complete depolarization of $\Delta\Psi_m$ occurred in the pH 6.9 medium (Figure 1C), as shown by little change after adding CCCP, and by the complete depolarization of $\Delta\Psi_m$ when Ca^{2+} recycling via the MCU was permitted (minus Ru360 group). Although adding CaCl_2 at an external pH_e of 6.9 led eventually to near complete dissipation of $\Delta\Psi_m$, when CsA was first added to the buffer, CsA prevented the gradual, slow extrusion of mCa^{2+} and declines in pH_m and $\Delta\Psi_m$ induced by adding CaCl_2 at pH_e 6.9 indicating a complete lack of CHE_m activity (see section “Supplementary Results S.2.1” and Supplementary Figures S.1A–C).

Increasing Matrix Acidification Led to Ca^{2+} Efflux Until Loss of the ΔpH_m Gradient and a Lack of Ca^{2+} Re-uptake via MCU on Full Depolarization of $\Delta\Psi_m$

A plot of extra-mitochondrial $[\text{Ca}^{2+}]_e$ as a function of matrix $[\text{H}^+]_m$ at each extra-mitochondrial pH (Figure 2) indicates maximal mCa^{2+} efflux occurred in the pH_e 6.9 medium (largest IMM (ΔH^+) gradient), much less so in the pH 7.15 medium, and not at all in the pH 7.6 medium. Ca^{2+} efflux was accentuated in the presence of Ru360 given just after the added CaCl_2 bolus (Figure 2). The difference (arrow) between the absence and presence of Ru360 indicates the rapid reuptake (recycling) of Ca^{2+} via MCU on extrusion via CHE_m . Thus total Ca^{2+} efflux was greater in the pH 6.9 group when MCU was not blocked because $[\text{H}^+]_m$ rose higher than when MCU was blocked. The steep, vertical increase in mCa^{2+} efflux at the highest $[\text{H}^+]_m$ in the pH 6.9 group resulted from cessation of mCa^{2+} reuptake via MCU due to depolarization of $\Delta\Psi_m$ (Figure 1C). The net amount of H^+ entering mitochondria per Ca^{2+} exiting mitochondria may be indeterminate because much of the H^+ entering is pumped out via the respiratory enzyme complexes.

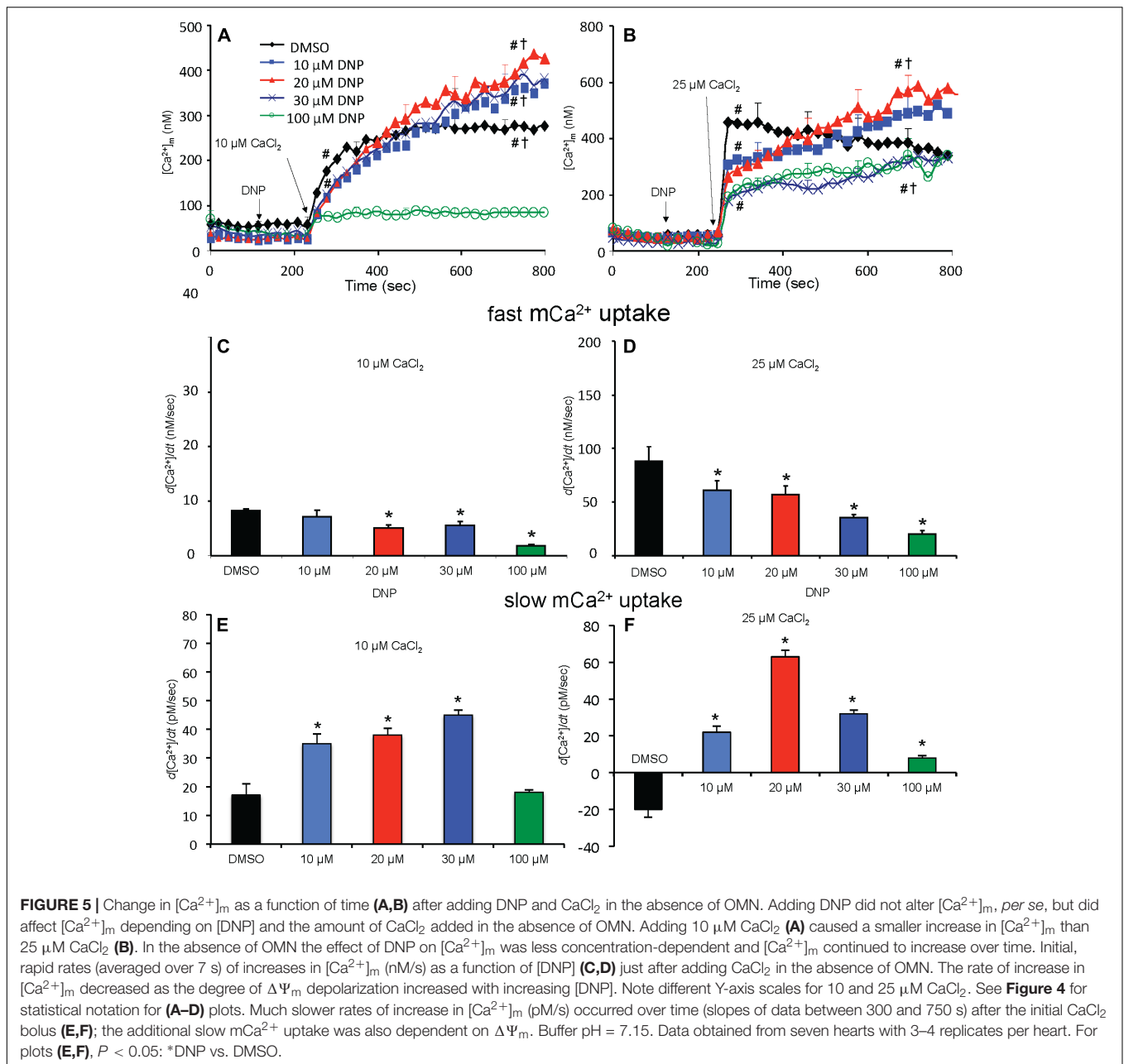
Mitochondrial Membrane Potential ($\Delta\Psi_m$) Was Depressed by DNP After Adding CaCl_2

In the protonophore series of experiments (time line, Figure 3), DNP alone decreased $\Delta\Psi_m$ slightly as assessed by rodamine-123

(R123) (Huang et al., 2007) (Figure 4), in a concentration-dependent manner, except at 100 μM DNP, which alone fully (+OMN) or nearly (–OMN) depolarized $\Delta\Psi_m$. $\Delta\Psi_m$ was estimated as % of maximal depolarization, where the baseline after adding substrate with OMN signifies full polarization (0%) and addition of CCCP denotes complete depolarization (100%). Adding 10 μL of 0.1% DMSO (DNP vehicle) or 10 μM DNP had no significant effect when given before CaCl_2 , whereas adding 20, 30, or 100 μM DNP before 10 μM CaCl_2 reduced the R123 $\Delta\Psi_m$ signals by 12.7, 18.7, and 92.4% vs. DMSO (Figure 4A), respectively. In the presence of OMN (Figure 4C), adding 20, 30, or 100 μM DNP before 10 μM CaCl_2 increased the fluorescence signal intensities (i.e., depolarized $\Delta\Psi_m$) by 16.2, 33.0, and 99.0%, respectively, vs. DMSO (0%). Overall, before adding either 10 or 25 μM CaCl_2 , 20 and 30 μM DNP moderately decreased $\Delta\Psi_m$ in the absence of OMN but greatly decreased $\Delta\Psi_m$ in the presence of OMN, suggesting blocked proton pumping from complex V (Figures 4C,D vs. Figures 4A,B). If no CaCl_2 was given after DNP, the moderate decrease in $\Delta\Psi_m$, which was unaffected by CsA, persisted for up to 25 min (see section “Supplementary Results S.2.5” and Supplementary Figure S.7A). After adding 10 and 30 μM DNP, and then CaCl_2 , there were large decreases in $\Delta\Psi_m$ resulting from entry of Ca^{2+} . Although $\Delta\Psi_m$ depolarization by DNP alone was unaffected by CsA, the subsequent slow $\Delta\Psi_m$ depolarization induced by 25 μM CaCl_2 was delayed by CsA (Supplementary Figure S.7B). Supplementary Results S.2.3 and Supplementary Figures S.3A–D shows statistics on mean \pm SEM data for $\Delta\Psi_m$ replotted from Figure 4 at time points 215, 275, and 700 s.

Matrix Free $[\text{Ca}^{2+}]_m$ Rose or Fell Slowly Depending on Block of Complex V

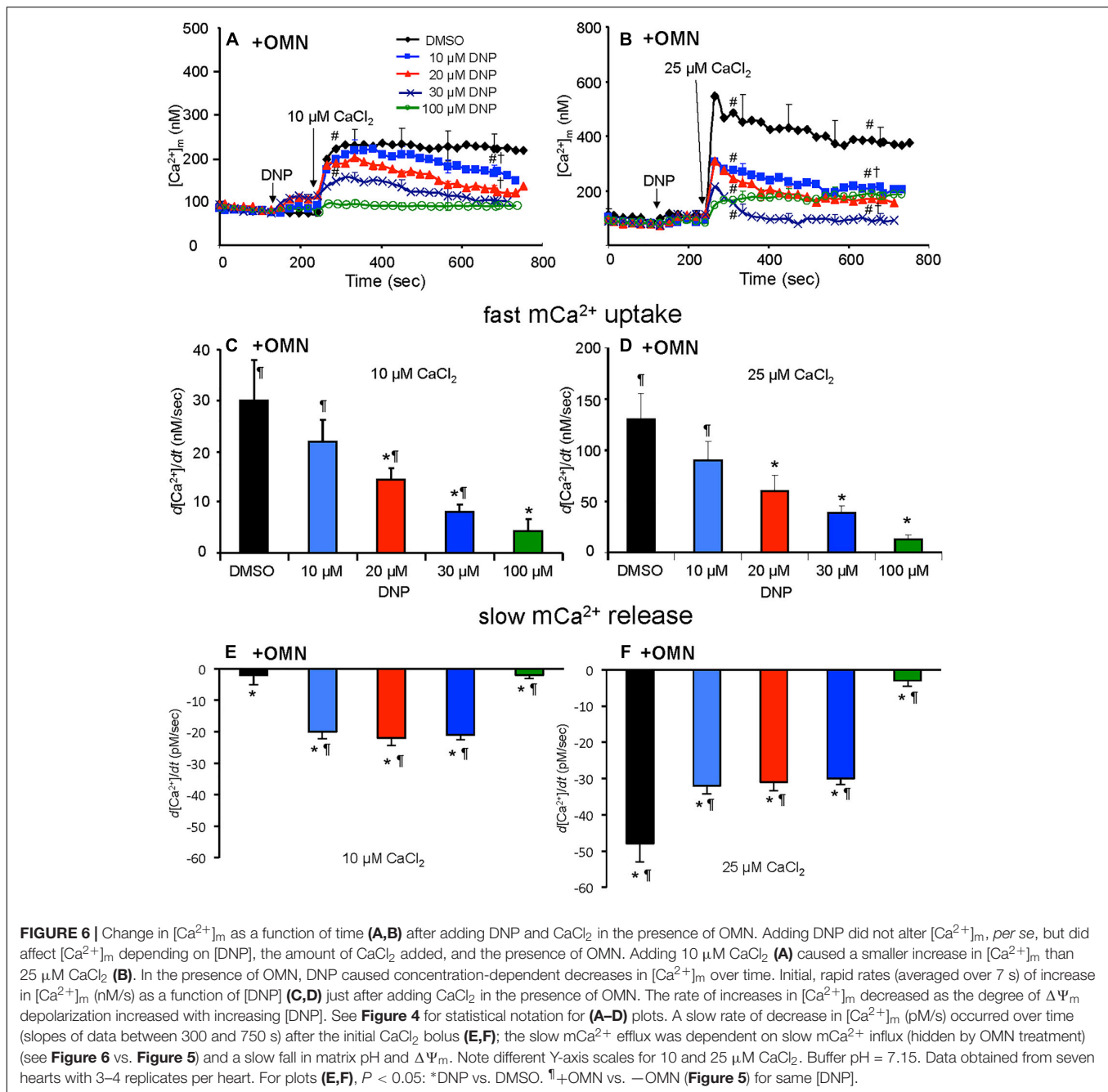
Adding 10 μM CaCl_2 without DNP ($\Delta\Psi_m$ fully polarized) caused $[\text{Ca}^{2+}]_m$ to increase rapidly from 80 nM (no added CaCl_2) initially to 235 nM at 300 s, whereas after adding 25 μM CaCl_2 , $[\text{Ca}^{2+}]_m$ rose more rapidly to 450 nM (Figures 5A,B); $[\text{Ca}^{2+}]_m$ remained unchanged over time (300–750 s) after adding 10 μM CaCl_2 but fell slightly and gradually (non-significantly) over time after adding 25 μM CaCl_2 (DMSO group, Figures 5A,B). After adding 10–30 μM DNP, adding 10 μM CaCl_2 promoted a slow, secondary rise in $[\text{Ca}^{2+}]_m$ (Figure 5A). The secondary, slow increase in $[\text{Ca}^{2+}]_m$ beginning 300 s after adding 10 μM CaCl_2 plus DNP was accompanied by a slow decrease in extra-mitochondrial $[\text{Ca}^{2+}]_e$ (see Supplementary Figure S.6A). When $\Delta\Psi_m$ was nearly or totally depolarized by 100 μM DNP in the absence of OMN, and after adding 10 μM CaCl_2 , there was no change in $[\text{Ca}^{2+}]_m$ over 300–750 s and thus no mCa^{2+} uptake over time (Figure 5A). $[\text{Ca}^{2+}]_m$ slowly increased over 300–750 s after first adding 10 and 20 μM DNP and then 25 μM CaCl_2 (Figure 5B), which caused the slow declines in $\Delta\Psi_m$ (Figure 4B). In the 100 μM DNP group $[\text{Ca}^{2+}]_m$ increased moderately immediately after adding 25 μM CaCl_2 , but did not change further over time. Supplementary Results S.2.6 and Supplementary Figures S.4A,B display statistics on



mean \pm SEM data for $[\text{Ca}^{2+}]_m$ replotted from Figure 5 (–OMN) at time points 215, 275, and 700 s.

In marked contrast, when complex V was blocked by OMN, adding 10 μM CaCl_2 (Figure 6A) after adding 10–30 μM DNP caused a marked decrease in $[\text{Ca}^{2+}]_m$ over time (300–750 s); after adding 25 μM CaCl_2 in the absence of DNP (Figure 6B), $[\text{Ca}^{2+}]_m$ rose higher initially, whereas 10–30 μM DNP caused a slow decrease in $[\text{Ca}^{2+}]_m$ over this period, indicating net mCa^{2+} efflux. Supplementary Results S.2.6 and Supplementary Figures S.4C,D shows statistics on mean \pm SEM data for $[\text{Ca}^{2+}]_m$ replotted from Figure 6 (+OMN) at time points 215, 275, and 700 s. The secondary, slow decrease in $[\text{Ca}^{2+}]_m$ after adding 20 μM DNP plus 25 μM CaCl_2 was accompanied by

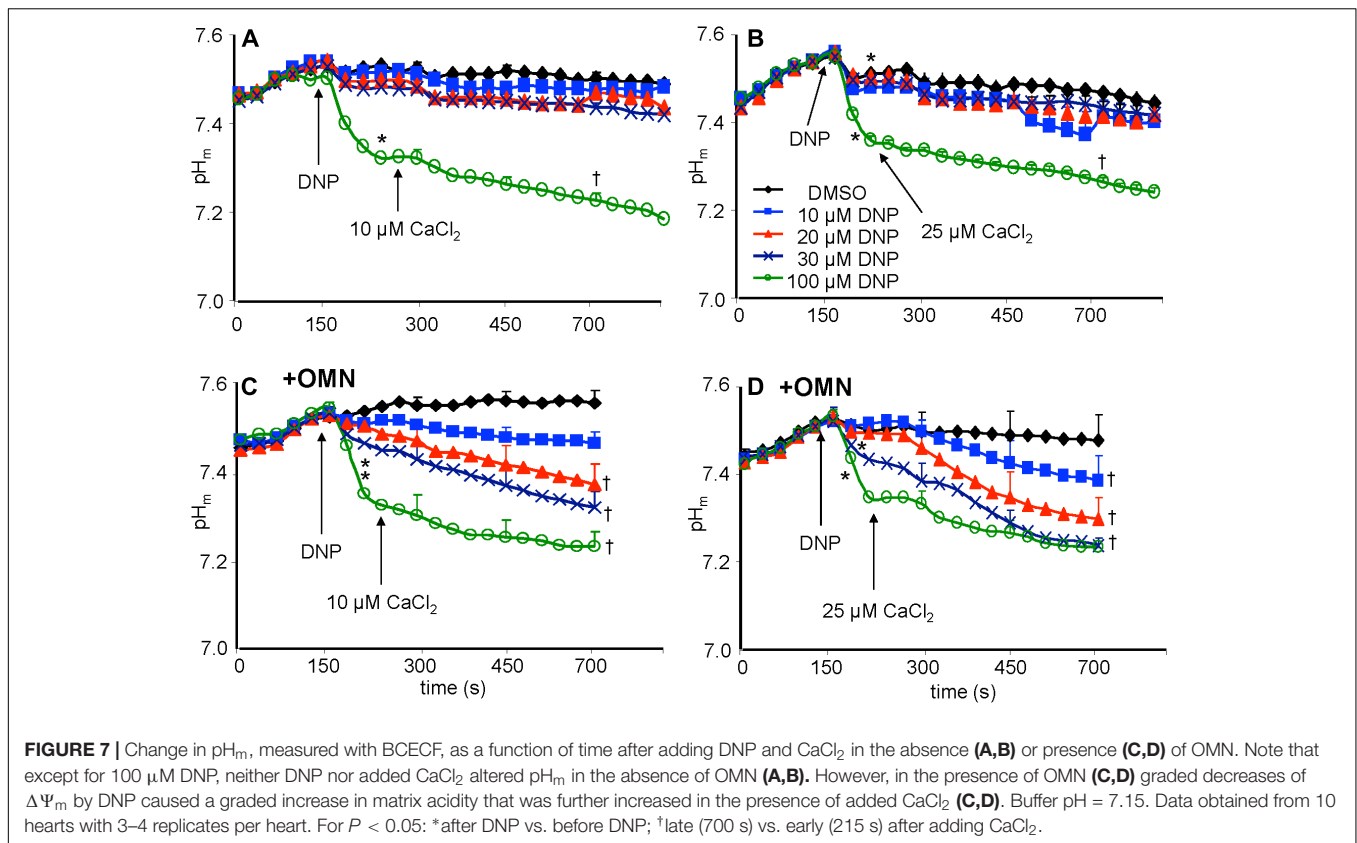
an increase in extra-mitochondrial $[\text{Ca}^{2+}]_e$ (see Supplementary Figure S.6B). Note that additional mCa^{2+} uptake after giving 25 μM CaCl_2 was halted after giving Ru360, 90 s later (at $t = 325$ s) and converted to mCa^{2+} efflux in the presence of OMN as shown by the increase in $[\text{Ca}^{2+}]_e$ (see Supplementary Figures S.6B vs. S.6A). A summary of slope data collected over the first 7 s (1 sample/s) after adding 10 or 25 μM CaCl_2 in the absence (Figures 5C,D) or presence (Figures 6C,D) of OMN shows that the average initial, rapid increase in $[\text{Ca}^{2+}]_m$ via the MCU was much faster after adding 25 μM CaCl_2 than after 10 μM CaCl_2 in the \pm OMN groups; this initial rate of mCa^{2+} uptake decreased as $\Delta\Psi_m$ fell with added DNP. The initial rate of increase in $[\text{Ca}^{2+}]_m$ during the first 7 s after



adding $10\ \mu\text{M}$ CaCl_2 (Figure 5C) decreased from 8 to 2 nM/s (DNP 0– $100\ \mu\text{M}$). After adding $25\ \mu\text{M}$ CaCl_2 (Figure 5D), the rate decreased from 88 to 20 nM/s. In the presence of OMN (Figures 6C,D), the initial increases in $[\text{Ca}^{2+}]_m$ in fully coupled mitochondria (no DNP) were larger than those in the absence of OMN (Figures 6C,D vs. Figures 5C,D). With OMN present, the initial increases in $[\text{Ca}^{2+}]_m$ decreased from 30 to 4 nM/s after adding $10\ \mu\text{M}$ CaCl_2 and from 130 to 13 nM/s after adding $25\ \mu\text{M}$ CaCl_2 . Thus the initial rates of increase in $[\text{Ca}^{2+}]_m$ with $10\ \mu\text{M}$ CaCl_2 were consistently faster in the presence of OMN (Figure 6C vs. Figure 5C), and at

$25\ \mu\text{M}$ CaCl_2 , with or without $10\ \mu\text{M}$ DNP (Figure 6D vs. Figure 5D).

A summary of slope data collected between 300 and 750 s, i.e., after the initial, rapid increase in $[\text{Ca}^{2+}]_m$ via the MCU with added $10\ \mu\text{M}$ CaCl_2 , demonstrates a much slower and smaller (pM/s) gradual increase in $[\text{Ca}^{2+}]_m$ over time in the absence of OMN with a threefold greater slope after $30\ \mu\text{M}$ DNP vs. DMSO (Figure 5E). After adding $25\ \mu\text{M}$ CaCl_2 , the slow increase in $[\text{Ca}^{2+}]_m$ was about fourfold higher after $20\ \mu\text{M}$ DNP vs. DMSO (Figure 5F). The secondary slow rise in $[\text{Ca}^{2+}]_m$ was about 1000 times slower than the initial fast phase and roughly dependent on



both the amount of mCa^{2+} that was taken up initially just after adding CaCl_2 and the extent of $\Delta\Psi_m$ depolarization. In contrast, in the presence of OMN under the same conditions of added CaCl_2 and DNP, the slope data showed slow and small declines (rather than increases) in $[\text{Ca}^{2+}]_m$ over time (Figures 6E,F). The slow rate of extrusion of mCa^{2+} by CHE_m when complex V was blocked with OMN (Figures 6E,F) became greater when mCa^{2+} entry via the MCU was greater (Figures 6 A,B).

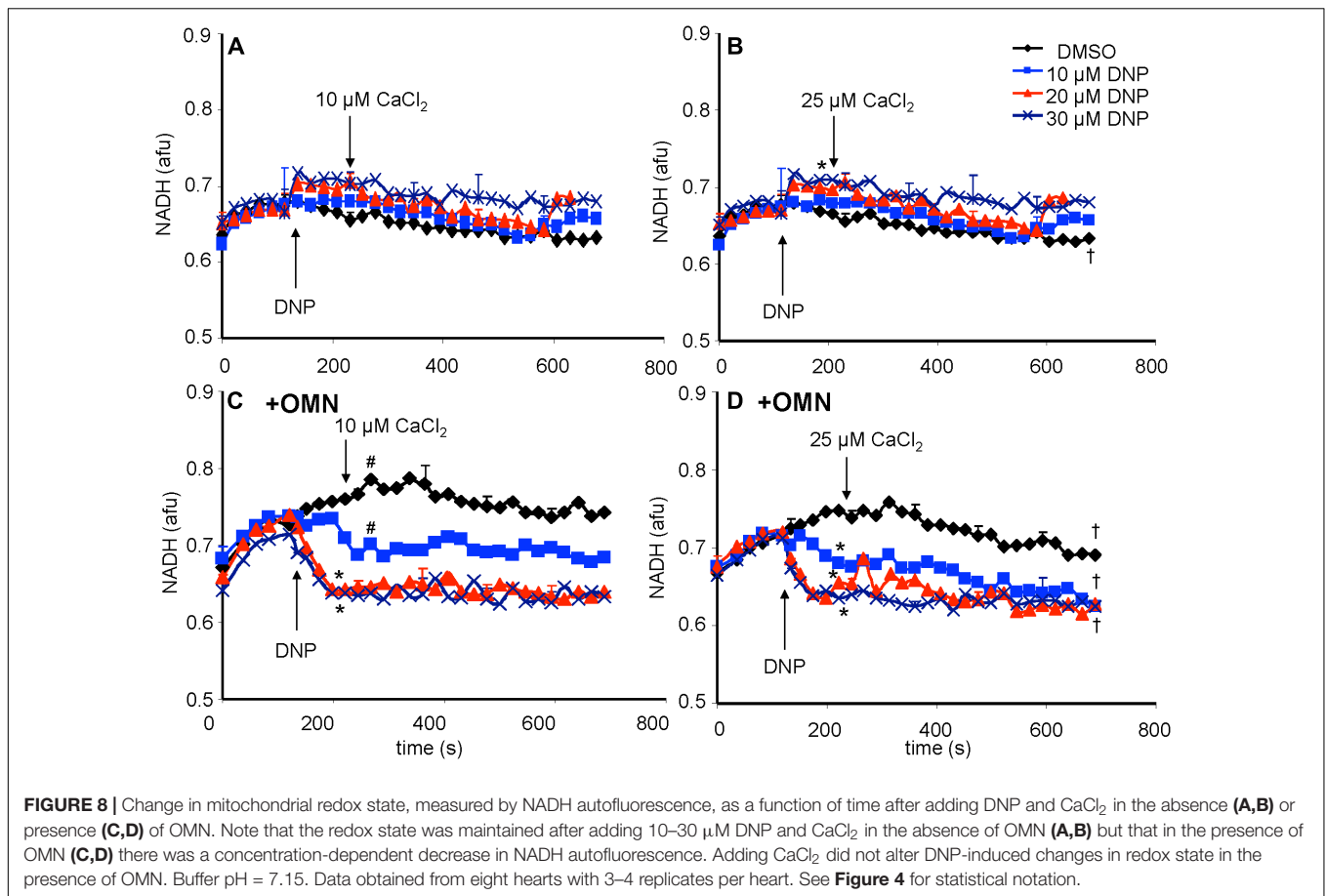
Matrix pH Remained Steady Without OMN but Fell With OMN-Induced Block of Complex V

Baseline matrix pH_m was approximately 7.55 in each group after adding PA and before adding DNP (Figures 7A–D). In the absence of OMN, adding 10–30 μM DNP did not result in a significant net decrease in pH_m ; however, 100 μM DNP markedly decreased pH_m (Figures 7A,B). This effect to collapse the ΔpH_m gradient was proportional to the collapse of the $\Delta\Psi_m$ gradient (Figure 4). In the absence of OMN, adding CaCl_2 had no appreciable effect on pH_m ($\Delta\Psi_m$ partially depolarized) even in the presence of DNP, except for 100 μM DNP, when pH_m fell markedly ($\Delta\Psi_m$ fully depolarized) (Figures 7A,B). In the absence of OMN, H^+ influx was matched by H^+ pumping as pH_m did not change appreciably. In contrast, in the presence of OMN there was a strong DNP concentration-dependent fall in matrix pH_m (Figures 7C,D) after adding CaCl_2 . This fall in pH_m was likely due to blocked H^+ pumping by

complex V in the presence of OMN (see below). **Supplementary Figures S.5A–D** shows statistics on mean \pm SEM data on pH_m replotted from Figure 7 (main text) at time points 215, 275, and 700 s. **Supplementary Figure S.8** displays plots of pH_m as a function of $[\text{Ca}^{2+}]_m$ at 700 s after adding DNP and CaCl_2 ; these correlations show how $[\text{Ca}^{2+}]_m$ decreases while pH_m decreases in the presence, but not in the absence of OMN.

Mitochondrial Redox State Remained Steady Without OMN but Fell With OMN-Induced Block of Complex V

A reduced redox state is associated with maintenance of pH_m . Adding the substrate PA increased the redox state (more reduced) as determined by high NADH autofluorescence (Figure 8). In the absence of OMN, adding 10 to 30 μM DNP \pm 10 or 25 μM CaCl_2 (Figures 8A,B) did not cause a significant change in NADH. NADH was unchanged despite up to 60% decrease in $\Delta\Psi_m$ fluorescence (Figures 4A,B) after adding DNP and CaCl_2 . However, when complex V was blocked by OMN (Figures 8C,D), there was significant oxidation (low NADH) by DNP in a concentration dependent manner. In contrast to the condition without OMN, with OMN present as little as a 20% fall in $\Delta\Psi_m$ fluorescence (Figures 4C,D) led to a more oxidized NADH state. Moreover, NADH was fully oxidized at 20 μM DNP with OMN present (Figures 8C,D), and the oxidized state was not altered significantly by adding CaCl_2 after DNP. In the absence or presence of CaCl_2 , NADH



was completely oxidized after adding 100 μM DNP (data not shown).

ATP Concentration Fell Without OMN but Remained Steady With OMN-Induced Block of Complex V

Total medium $[\text{ATP}]$ was measured and mitochondrial $[\text{ATP}]_m$ was estimated (see section “**Supplementary Materials S.1.10**”). Basal $[\text{ATP}]_m$ was measured after adding mitochondria to the experimental buffer in the absence of OMN (**Figures 9A,B**). There was no change in basal $[\text{ATP}]_m$ after adding PA. DNP, at 10 μM , did not significantly change $[\text{ATP}]$ before or after adding CaCl_2 (**Figures 9A,B**). Basal $[\text{ATP}]_m$ was unchanged if CaCl_2 was not added (data not displayed). Adding 20 or 30 μM DNP alone had no significant effect on $[\text{ATP}]_m$, but adding CaCl_2 resulted in a decrease in $[\text{ATP}]_m$ (**Figures 9A,B**). In the presence of OMN (**Figures 9C,D**), adding mitochondria to the buffer did not change $[\text{ATP}]_m$, indicating inhibited complex V activity. $[\text{ATP}]_m$ remained at a very low level and was unaffected by DNP or CaCl_2 in the presence of OMN. With OMN present, $\text{ATP}_m/\text{ADP}_m$ ratios (see section “**Supplementary Materials S.1.11, S.1.12 and Supplementary Results S.2.9**”) also decreased with added DNP and CaCl_2 , along with the progressive declines in $\Delta\Psi_m$.

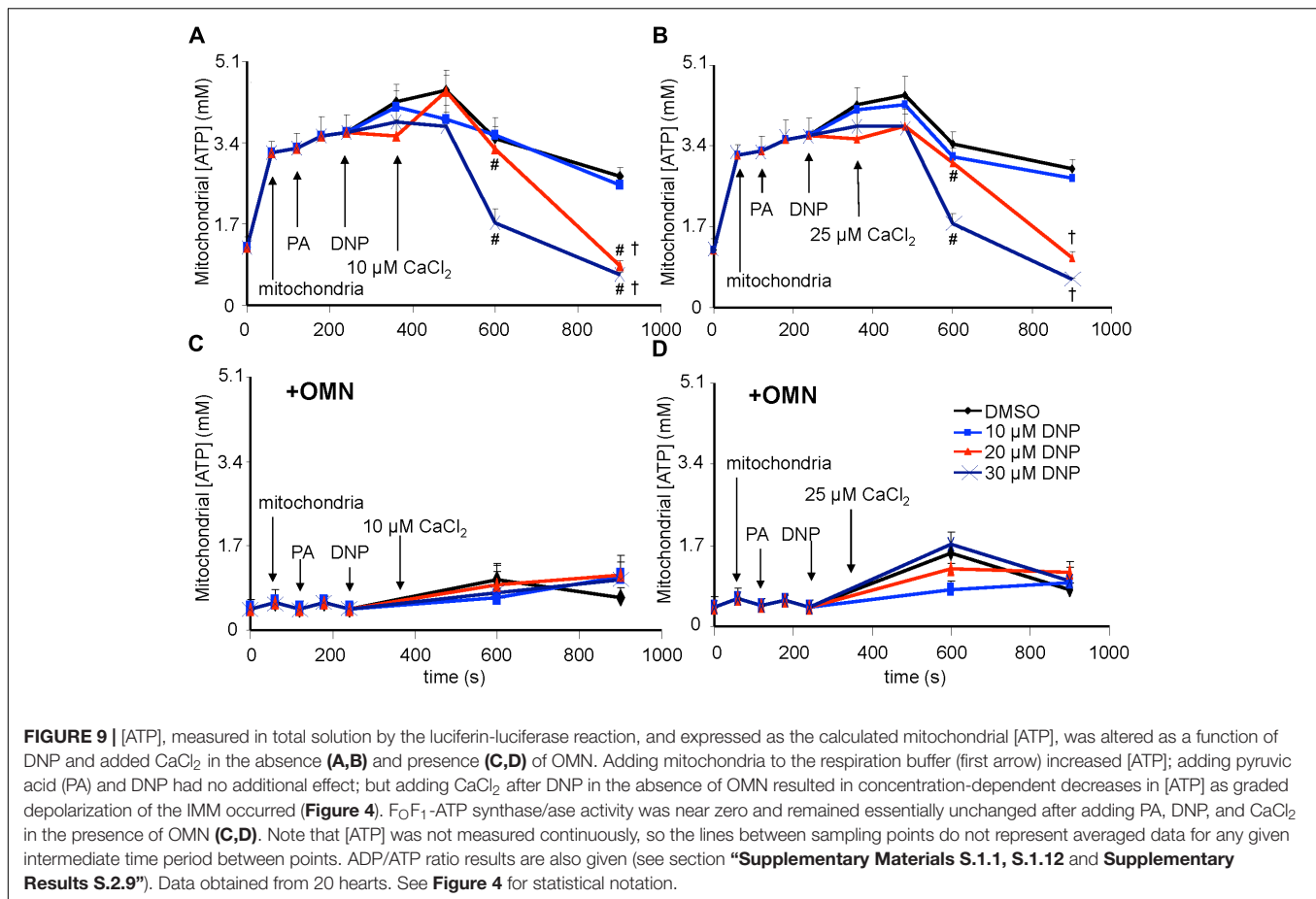
Additional Supplemental Comparisons and Calculations

Supplementary Results S.2.2 and **Supplementary Figure S.2** demonstrate the effect of adding DNP and CaCl_2 on respiration. **Supplementary Results S.2.7** and **Supplementary Figure S.9** furnish values for $\Delta\Psi_m$, $[\text{Ca}^{2+}]_m$, and pH_m at 700 s, replotted from **Figures 4–7**, to compare these results in the presence or absence of OMN. The **Supplementary Table** shows DNP concentrations that produced 50% inhibitions (IC_{50}) of $\Delta\Psi_m$, $[\text{Ca}^{2+}]_m$, fast (initial) $d[\text{Ca}^{2+}]_m/dt$, and pH_m as a linear function of 0–30 μM DNP \pm OMN at the 700 s time point. **Supplementary Figure S.10** displays calculated mCa^{2+} flux rates (J_{CHE}) for CHE_m (see section “**Supplementary Results S.2.8**”) in the absence and presence of OMN.

DISCUSSION

$\text{Ca}^{2+}/\text{H}^+$ Exchange Activity Is Identified by Manipulating IMM $\Delta[\text{H}^+]$ and $\Delta[\text{Ca}^{2+}]$ Gradients

We provide firm support for a role of CHE_m in maintaining homeostasis of Ca^{2+} against H^+ under certain conditions in cardiac cell mitochondria that may mimic some sequelae of



cardiac IR injury. Our results: (1) furnish direct evidence for CHE_m activity by the secondary, slow increases in matrix Ca^{2+} efflux coupled to slow increases in matrix H^+ influx, when both NCE and NHE activities are blocked, and particularly, when MCU-dependent mCa^{2+} re-uptake is blocked with Ru360; (2) demonstrate that respiration increases while $\Delta\Psi_m$ decreases mildly, whereas pH_m and redox state are relatively maintained when inducing a matrix inward H^+ leak with DNP before adding CaCl_2 ; adding CaCl_2 results in a secondary, slow increase in $[\text{Ca}^{2+}]_m$ that slowly depolarizes $\Delta\Psi_m$; (3) show that with permissive H^+ influx, but inhibited outward H^+ pumping at complex V, adding CaCl_2 causes larger decreases in $\Delta\Psi_m$, pH_m , and NADH and results in a slow decrease in $[\text{Ca}^{2+}]_m$; (4) indicate that blocking complex V with OMN to prevent H^+ pumping causes $\Delta\Psi_m$ to further decrease after adding CaCl_2 because the influx of mCa^{2+} via the MCU is not opposed by H^+ pumping at complex V; (5) suggest that the lack of a slow fall or rise in $[\text{Ca}^{2+}]_m$ in the presence of $100 \mu\text{M}$ DNP is due to the loss of $\Delta\Psi_m$ -dependent mCa^{2+} uptake by MCU; (6) point out that only in partially depolarized mitochondria does added CaCl_2 result in a pH_m -independent gradual increase in $[\text{Ca}^{2+}]_m$ that is reciprocated by H^+ pumping to maintain pH_m ; preventing matrix acidification is associated with a maintained redox state; and (7) show that the decrease in [ATP] in the absence of

OMN supports ATP hydrolysis with H^+ pumping. These two scenarios, $\pm\text{OMN}$, are depicted graphically in **Figure 10A** vs. **Figure 10B**.

Net Mitochondrial Ca^{2+} Influx Occurs via MCU and Net Ca^{2+} Efflux Can Occur via $\text{Ca}^{2+}/\text{H}^+$ Exchange

The dependence of rapid MCU-mediated mCa^{2+} uptake on $\Delta\Psi_m$ has been examined extensively (Gunter and Pfeiffer, 1990; Gunter et al., 1994; Dash et al., 2009; Haumann et al., 2010). But our study demonstrates that net $\text{m}[\text{Ca}^{2+}]$ can additionally increase slowly via the MCU, and that this happens when pH_m is relatively maintained despite a decline in $\Delta\Psi_m$ resulting from the DNP-mediated inward H^+ flux and after the initial rapid Ca^{2+} influx via MCU. A gradual increase in $[\text{Ca}^{2+}]_m$ at the expense of maintaining the ΔpH_m may be deleterious to mitochondrial function. We propose that this secondary rise in net $[\text{Ca}^{2+}]_m$ results from an adequate $\Delta\Psi_m$ with Ru360-dependent slow mCa^{2+} influx, which eventually leads to a slow, continued fall in $\Delta\Psi_m$. Because H^+ pumping at complex V maintains the $\Delta[\text{H}^+]_m$ gradient, mCa^{2+} efflux via CHE_m in exchange for mH^+ influx due to the H^+ leak is likely masked by mCa^{2+} re-uptake. Thus, the DNP-induced H^+ leak and the concomitant dissipation of the IMM $\Delta[\text{H}^+]$ gradient, when

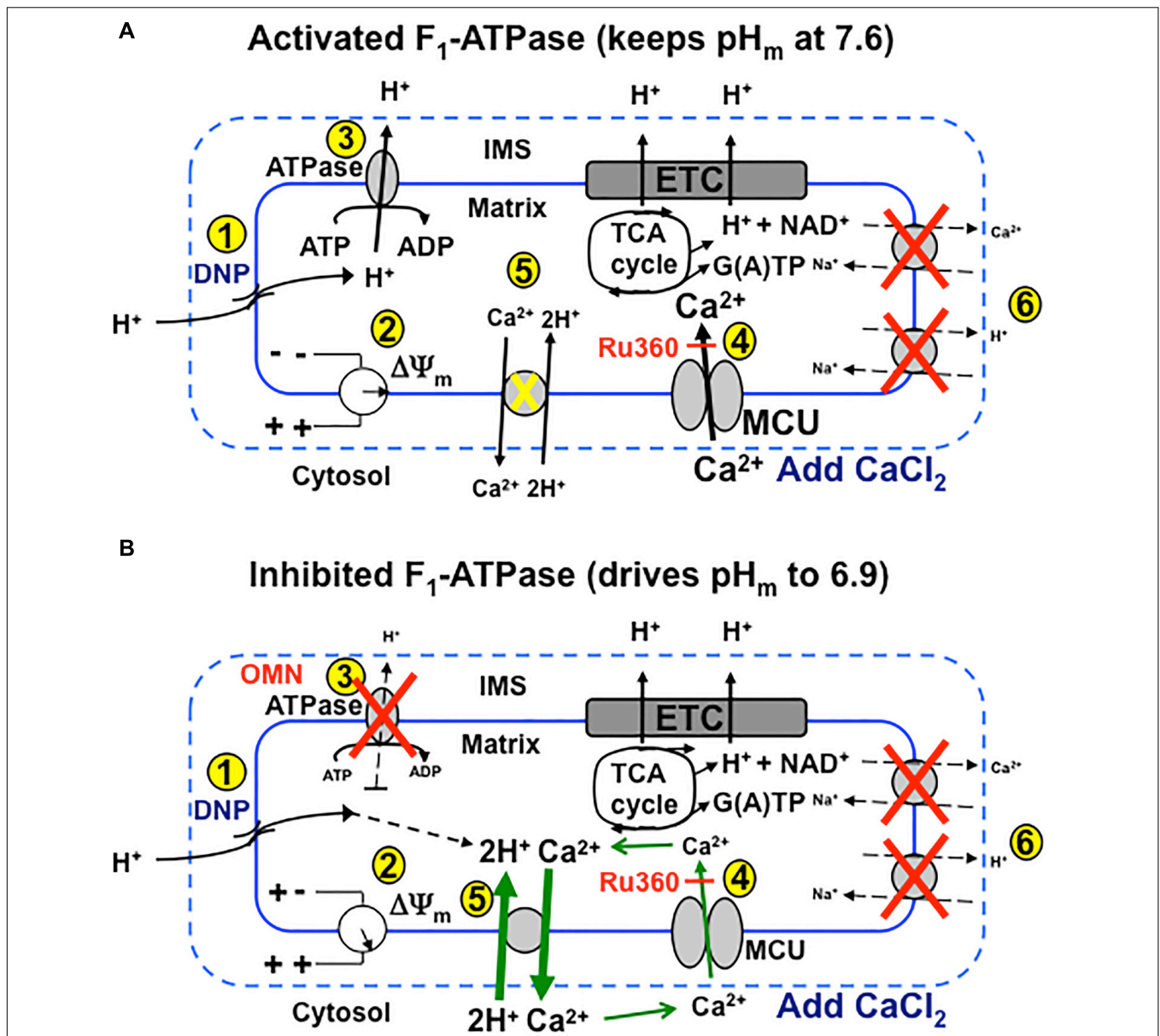


FIGURE 10 | Schema depicting putative role of MCU and CHE_m on slow Ca^{2+} influx and efflux, respectively, during stepwise depolarization with DNP with un-inhibited (i.e., minus OMN) (A) vs. inhibited (B) F_0F_1 -ATP synthase (i.e., plus OMN) after a bolus addition of CaCl_2 to the mitochondrial medium. (A) (1) DNP permits H^+ entry that tends to (2) decrease $\Delta\Psi_m$, which enhances H^+ pumping by respiratory complexes, including (3) F_0F_1 -ATPase, so that pH_m does not decrease appreciably and $\Delta\Psi_m$ is partially supported (2). Adding CaCl_2 further depolarizes $\Delta\Psi_m$ by allowing more cationic (Ca^{2+}) charges into the matrix via the MCU (4). Over time, in the range of a 20–60% decline in $\Delta\Psi_m$, pH_m remains unchanged as (5) H^+ is pumped out (3) in exchange for permissive H^+ entry (1) in triggering additional slow mCa^{2+} uptake by MCU and causing $\Delta\Psi_m$ to decrease further. CHE_m is inhibited by the lack (pH 7.6) of matrix acidity (5) and NCE_m and NHE_m are inactivated by the lack of substrate and buffer Na^+ (6). (B) Alternatively, when F_0F_1 -ATPase is inhibited (3), matrix acidity gradually increases (pH 6.9), $\Delta\Psi_m$ is less supported (2) and Ca^{2+} slowly exits (CHE_m) in exchange for slow H^+ entry due to DNP (5). This sequence triggers a net loss of mCa^{2+} even though uptake of Ca^{2+} via the MCU continues, as shown by a greater efflux of mCa^{2+} by CHE_m when additional mCa^{2+} uptake via MCU is blocked by Ru360 (4). DNP, dinitrophenol; ETC, electron transport chain; IMS, inner membrane space; MCU, mitochondrial Ca^{2+} uniporter; OMN, oligomycin; TCA, tricarboxylic acid.

countered by H^+ pumping at complex V (in addition to other complexes), can maintain the ΔpH_m and support the pmf ($\Delta\Psi_m + RT/F\Delta\text{pH}_m$) (Dzбек and Korzeniewski, 2008). This view is especially supported by the smaller decline in extra-mitochondrial $[\text{Ca}^{2+}]_e$ in the presence of 20 μM DNP, 25 μM CaCl_2 , and OMN, as well as in the presence of Ru360, by

the gradual increase in $[\text{Ca}^{2+}]_e$ due to CHE_m mediated Ca^{2+} efflux. These results are reinforced by the exaggerated effect of added CaCl_2 to enhance the decline in $\Delta\Psi_m$ over time and by the slow decreases in $[\text{Ca}^{2+}]_m$ linked to slow decreases in pH_m . Blocking outward H^+ pumping by complex V prevented compensation for DNP-mediated H^+ influx. Consistent with

our observations, it was reported that matrix acidification may reduce Ca^{2+} uptake in cardiac mitochondria by its effect on decreasing $\Delta\Psi_m$ (Gursahani and Schaefer, 2004). In contrast, when ATP_m hydrolysis is prevented, pH_m slowly decreases toward pH_e with a greater fall in $\Delta\Psi_m$; the slow H^+ influx is accompanied by a slow net fall in $[\text{Ca}^{2+}]_m$ mediated by CHE_m even though the extruded Ca^{2+} is recycled via the MCU. Since H^+ influx (DNP-induced leak) is not countered by reciprocal H^+ pumping to restore ΔpH_m , the slow influx of H^+ is exchanged for slow Ca^{2+} efflux via CHE_m until the ΔpH gradient is dissipated.

Ca^{2+} and H^+ gradients across the IMM are largely dependent on $\Delta\Psi_m$ and ΔpH gradients resulting from H^+ pumping by respiratory complexes. Ionic homeostasis requires one cation efflux pathway to oppose another cation influx pathway and *vice versa*. Cation exchangers fulfill this need. Unlike mCa^{2+} uptake via MCU, which is dependent on $\Delta\Psi_m$ and on the chemical gradient, exchange of Ca^{2+} and H^+ via CHE_m may or may not be dependent on $\Delta\Psi_m$ (Rottenberg and Marbach, 1990; Gunter et al., 1991). But the direction of Ca^{2+} and H^+ flux mediated solely by CHE_m is dependent on a large IMM $[\text{H}^+]$ or $[\text{Ca}^{2+}]$ gradient to shuttle Ca^{2+} or H^+ across the IMM. This can be expressed by an electroneutral J_{CHE} flux equation (Tewari et al., 2014), calculated here in the presence and absence of OMN (see section “Supplementary Results S.2.8” and Supplementary Figure S.10). J_{CHE} flux analysis of our data suggests that slow mCa^{2+} influx could have occurred via CHE_m in the absence of OMN, whereas mCa^{2+} efflux could have occurred in the presence of OMN. Indeed, we have provided strong support for slow net mCa^{2+} efflux mediated by CHE_m (despite slow mCa^{2+} uptake by MCU) when complex V cannot pump H^+ in the presence of OMN.

Although CHE_m likely occurs both in the absence or presence of OMN, our results suggest that the observed secondary, slow influx of mCa^{2+} influx (minus OMN) is due primarily to re-uptake by a Ru360 sensitive mechanism, presumably MCU, that may overwhelm any CHE_m activity. This is because Ru360 blocked the slow rise in $[\text{Ca}^{2+}]_m$ and the slow fall in $[\text{Ca}^{2+}]_e$, thus supporting MCU as the mediator of the slow mCa^{2+} influx. The J_{CHE} flux equation only monitors differences in $[\text{H}^+]$ and $[\text{Ca}^{2+}]$ on either side of the IMM and does not rely on effects of the ΔpH_m gradient on H^+ pumping or the $\Delta\Psi_m$ gradient on mCa^{2+} uptake via MCU. Thus the secondary, slow mCa^{2+} uptake after the initial CaCl_2 bolus (Figures 5A,B,E,F) appears to be a direct effect of H^+ pumping by complex V (minus OMN) to maintain the ΔpH_m charge gradient and support the *pmf* although $\Delta\Psi_m$ continues to fall due to the continued mCa^{2+} influx. On the other hand, inhibiting ATP_m hydrolysis (Figures 9C,D) to prevent H^+ pumping not only enhances the fall in $\Delta\Psi_m$ (Figures 4C,D) to retard further mCa^{2+} loading by the MCU, but also permits slow CHE_m -mediated mCa^{2+} efflux (Figures 6A,B,E,F) in exchange for mH^+ influx until the diminishing ΔpH_m gradient is abolished (Figures 7C,D).

Alternatively, we demonstrated CHE_m activity by acidifying the external medium before adding CaCl_2 , while blocking NCE_m and NHE_m activities by using Na^+ free buffer and substrates. We observed a slowly increasing $[\text{Ca}^{2+}]_e$ coupled to a slowly

increasing $[\text{H}^+]_m$. We used Ru360 to expose the net amount of mCa^{2+} efflux via CHE_m by blocking the effluxed Ca^{2+} from re-entering via MCU (Figures 1, 2). It is unlikely that 0.1–1 μM Ru360 inhibits CHE_m because Ru360 did not block mCa^{2+} efflux (Figures 1, 2), only mCa^{2+} influx. Of course, Ru360 might block another mode of non-MCU Ca^{2+} uptake. Our proposed mechanism is described schematically in Figures 10A,B. We postulate that CHE_m activity is completely inhibited if the matrix remains alkaline (large ΔpH_m gradient), thus exposing net Ca^{2+} uptake via MCU. The slow increases in $[\text{Ca}^{2+}]_m$ that we observed previously (Haumann et al., 2010) likely represent net slow mCa^{2+} via MCU (reference Figure 5).

A leucine zipper EF hand-containing trans-membrane protein (LETM1) found in non-mammalian cells is thought to be a molecular component of CHE_m (Jiang et al., 2009; Shao et al., 2016). Knockdown and expression of LETM1 in a number of cell lines support its role in $\text{Ca}^{2+}/\text{H}^+$ exchange, particularly in mitochondria (Jiang et al., 2013; Doonan et al., 2014). Alternatively, other studies (Nowikovsky et al., 2004, 2012; Froschauer et al., 2005; Malli and Graier, 2010; Austin et al., 2017) support that LETM1 either does not mediate Ca^{2+} efflux (De Marchi et al., 2014) or that it mediates K^+/H^+ and/or Na^+/H^+ exchange, so conclusive genetic evidence for CHE requires more study. It is important to note that the elusive CHE protein appears to be insensitive to MCU inhibitors, i.e., ruthenium red (RR) compounds (Bernardi et al., 1984), and to CGP-37157, the NCE inhibitor (Tsai et al., 2014). The present study explores for the first time the kinetics of CHE_m activity in relation to MCU activity in cardiac cell mitochondria.

$\Delta\Psi_m < E_{\text{REV-ATPase}}$ Promotes ATP Hydrolysis

F_0F_1 -ATPsynthase/ase directionality is governed by $\Delta\Psi_m$ and its “reversal potential” $E_{\text{REV-ATPase}}$, which in turn is dependent on the concentration of the reactants ATP/ADP , and H^+ (Metelkin et al., 2009; Chinopoulos and Adam-Vizi, 2010; Chinopoulos et al., 2010). Additional factors of E_{REV} that affect the direction and rate of ATP synthesis/hydrolysis are the free $[\text{P}_i]$ and the $\text{H}^+_m/\text{ATP}_m$ coupling ratio, n (Cross and Muller, 2004). When $\Delta\Psi_m$ becomes less negative than E_{REV} , which depends on a high $[\text{ATP}]_m$ and ΔpH_m , but a low $[\text{ADP}]_m$, H^+ ejection by complex V becomes thermodynamically favorable (Metelkin et al., 2009; Chinopoulos and Adam-Vizi, 2010; Chinopoulos et al., 2010; Chinopoulos, 2011). $E_{\text{REV-ATPase}}$ can occur when $\Delta\Psi_m$ falls between -130 and -100 mV, depending on matrix $[\text{ATP}]_m/[\text{ADP}]_m$, $[\text{P}_i]_m$, ΔpH_m , and the coupling ratio (Chinopoulos et al., 2010; Chinopoulos, 2011). Others (Leysens et al., 1996; Bains et al., 2006; Chinopoulos and Adam-Vizi, 2010) have observed that a fall in $\Delta\Psi_m$ caused by a protonophore, such as DNP or CCCP, can induce ATP hydrolysis through reversal of F_0F_1 -ATPsynthase. The consequent H^+ pumping by complex V would tend to partially restore $\Delta\Psi_m$ to offset the protonophore-induced decreases in pH_m and $\Delta\Psi_m$ as discussed above. The electrical gradient $\Delta\Psi_m$ and the H^+ chemical gradient $\Delta[\text{H}^+]_m$ together contribute to the total *pmf* that powers the synthesis of ATP; when *pmf* is not maintained, hydrolysis of matrix ATP

occurs. Previous studies have also furnished indirect evidence for reversal of F_0F_1 -ATP synthase under conditions of reduced mCa^{2+} uptake and a fully depolarized $\Delta\Psi_m$ with CCCP (Leyssens et al., 1996; Bains et al., 2006). ATP_m hydrolysis has been reported to occur *in vivo* during cardiac ischemia (Grover et al., 2004), but the *in vivo* $\Delta\Psi_m$ at which this occurs is not known. Here we show how a DNP-induced fall in $\Delta\Psi_m$ induces ATP hydrolysis.

In the absence of OMN, the lack of a fall in ATP levels after adding 10 μM DNP indicated that ATP_m hydrolysis (Figure 9) did not occur because $\Delta\Psi_m$ remained relatively stable before adding CaCl_2 . However, adding CaCl_2 resulted in a gradual, but large, fall in $\Delta\Psi_m$ over time. In the presence of 20 μM DNP and 25 μM CaCl_2 , ATP hydrolysis occurred (20–25% of maximum) with a decrease in $\Delta\Psi_m$ at an IMM gradient of approximately 0.35 ΔpH_m units (Figures 7A,B). A faster rate of ATP hydrolysis was indicated by the additional fall in $[\text{ATP}]_m$ over time after adding 30 μM DNP and CaCl_2 . The DNP-induced falls in $\Delta\Psi_m$ were accompanied by reduced $\text{ATP}_m/\text{ADP}_m$ ratios (see section “Supplementary Materials S.1.11, S.1.12 and Supplementary Results S.2.9”) indicating consumption of ATP , as also shown by the lower $[\text{ATP}]_m$ (Figures 9A,B). A calculation of available matrix ATP is given (see section “Supplementary Results S.2.10”). In the presence of 100 μM DNP and added CaCl_2 , $\Delta\Psi_m$ was maximally depolarized (Figures 4A,B), the ΔpH_m gradient was abolished (Figures 7A,B), and NADH was oxidized (Figures 8A,B), indicating that ATP_m hydrolysis was insufficient to maintain the *pmf*. This contrasts to the situation with 10–30 μM DNP where *pmf* was supported largely by the ΔpH_m gradient, as also reflected by the maintained NADH redox state.

$\Delta\Psi_m$ is normally fully polarized when complex V is blocked by OMN (Valdez et al., 2006; Brand and Nicholls, 2011); however, the effect of DNP to slightly decrease $\Delta\Psi_m$ was intensified when OMN was present, particularly after adding 25 μM CaCl_2 that intensifies the depolarization of $\Delta\Psi_m$ in the presence of DNP. This effect of DNP in the absence of OMN indicates that ATP hydrolysis indeed supported the ΔpH_m via H^+ pumping even at a relatively small decline in $\Delta\Psi_m$ with DNP. With OMN present, ATP hydrolysis cannot occur (Figures 9C,D) and so complex V cannot contribute to maintaining pH_m ; therefore, the low pH_m accompanied by a high $[\text{Ca}^{2+}]_m$ must have activated CHE_m .

Changes in pH_m , $[\text{Ca}^{2+}]_m$, and NADH Are Larger With OMN Than Without OMN

An interesting observation of our study is the contribution of complex V to maintain the ΔpH_m gradient (and thus supporting the *pmf*) whereby the H^+ leak is compensated by augmented H^+ pumping by complex V; this resulted in slow mCa^{2+} influx (“ Ca^{2+} leak”) that could be blocked by Ru360, which indicates the influx likely occurred via MCU. But if compensatory H^+ pumping is blocked by OMN, the matrix becomes acidic, the ΔpH_m gradient falls lower, and slow mCa^{2+} efflux occurs via CHE_m thus masking the slow mCa^{2+} influx (Figure 10B). Evidence for H^+ pumping during ATP hydrolysis during DNP-mediated H^+ influx was provided by the maintenance of an alkaline pH_m ; moreover, pH_m indeed

fell when H^+ pumping was blocked by OMN. Similarly, if mitochondria reside in an acidic environment (Figures 1, 2), $[\text{H}^+]_m$ falls as $[\text{Ca}^{2+}]_e$ rises, indicating CHE_m . Indeed, in a previous study it was reported that adding lactic acid to a Na^+ free mitochondrial suspension increased buffer Ca^{2+} by 43% (Gambassi et al., 1993); it was suggested that Ca^{2+} was extruded as H^+ influx caused H^+ ions to compete with Ca^{2+} ions for mitochondrial binding sites (Gambassi et al., 1993). We furnish direct evidence for a link between Ca^{2+} efflux with H^+ influx in mammalian cardiac muscle mitochondria, when Na^+ is absent and the MCU is blocked after adding CaCl_2 .

NADH levels remained unchanged after adding DNP and CaCl_2 (Figures 8A,B); this likely reflects the faster state 2 respiration (Supplementary Figure S2) since the inward H^+ leak by DNP was balanced by H^+ pumping from complex V as well as from complexes I, III, and IV. Only at 100 μM DNP with CaCl_2 , which fully depolarized $\Delta\Psi_m$ (Figures 4A,B), did DNP result in a lower pH_m (Figures 7A,B) and a more oxidized redox state, i.e., a decrease in NADH (Figures 8A,B). It is likely that an increase in F_0F_1 -ATPase activity plus a faster TCA cycle turnover (increased NADH/NAD^+ ratio) can result in maintained NADH levels despite the DNP-induced H^+ leak. In the presence of OMN, however, NADH was gradually oxidized (Figures 8C,D) along with the fall in pH_m (Figures 7C,D); this scenario likely occurred because the additional H^+ pumping by complex V to support $\Delta\Psi_m$ was blocked. We observed that adding CaCl_2 alone did not significantly change NADH levels in this model, which is consistent with our earlier study (Haumann et al., 2010). Although an increase in $[\text{Ca}^{2+}]_m$ can stimulate NADH producing dehydrogenases (Denton et al., 1980; McCormack and Denton, 1980; Wan et al., 1989; Brandes and Bers, 1997), our experiments were conducted at maximal $[\text{Ca}^{2+}]_m$ values below the $K_{0.5}$ of 1 μM Ca^{2+} at which these dehydrogenases are reported to be activated (Denton et al., 1980; McCormack and Denton, 1980).

What Is the Functional Role of CHE_m : How Is Net mCa^{2+} Efflux Modified by mCa^{2+} Influx via MCU?

The net Ca^{2+} driving force for ions across the IMM can be estimated by Nernst equilibrium potentials for given estimates of $\Delta\Psi_m$. Under conditions of 20 μM DNP, 25 μM CaCl_2 , and in the absence of OMN, when $[\text{Ca}^{2+}]_m$ slowly increased, we calculated Nernst equilibrium potentials of approximately -8 and $+18$ mV, respectively, for $[\text{Ca}^{2+}]$ and $[\text{H}^+]$ at 700 s. We estimated $\Delta\Psi_m$ as -110 to -120 mV at 700 s (based on our values for % of minimal and maximal depolarization (R-123 fluorescence) and curve fitting for approximating conversion to $\Delta\Psi_m$ (Huang et al., 2007)). This indicated that the driving force for both Ca^{2+} and H^+ would remain inward despite H^+ pumping at complex V to attempt to re-establish the ΔpH_m gradient by compensating for the DNP-mediated H^+ influx. Based on our estimated $\Delta\Psi_m$ and the calculated Ca^{2+} and H^+ equilibrium potentials driving both Ca^{2+} and H^+ inward, we conclude that the outward H^+ pumping by complex V (in addition to complexes I, III, IV) was

sufficient to compensate for the continued inward influx of H^+ mediated by DNP thus restoring the ΔpH_m gradient, but not the *pmf*, and thus preventing activation of CHE_m . Ru360 blocked this additional uptake of mCa^{2+} by the MCU so that $[\text{Ca}^{2+}]_e$ did not continue to fall.

We predict that the major conduit for both fast and slow mCa^{2+} influx under our experimental conditions occurs primarily via the MCU. The efflux of Ca^{2+} via the CHE_m is slow so we expect the re-uptake of Ca^{2+} via the MCU also would be slow. Although the J_{CHE} flux equation alone predicted that slow mCa^{2+} influx could have occurred via CHE_m this is unsustainable if $[\text{H}^+]_m < [\text{H}^+]_e$. It is likely that voltage-dependent transport of net Ca^{2+} inward is mostly responsible if there is at least a partially maintained $\Delta\Psi_m$ (Nernst potentials) despite mCa^{2+} extrusion via CHE_m . Interestingly, under the condition of a fully polarized $\Delta\Psi_m$ (no DNP and no OMN) (Figures 4A–D), $[\text{Ca}^{2+}]_m$ did not rise as it did in the presence of DNP (Figures 5A,B) when pH_m was maintained (Figures 7A,B). This suggests that the secondary, slow uptake of mCa^{2+} is indirectly related to H^+ pumping due to the decline in $[\text{H}^+]_m$ to support the *pmf*; the additional, slow mCa^{2+} uptake by the MCU occurs because of the remaining charge gradient ($\Delta\Psi_m$) and Ca^{2+} chemical gradient.

In contrast, in the presence of OMN the kinetics of the delayed, slow mCa^{2+} efflux via CHE_m under conditions of reduced $\Delta\Psi_m$ and low pH_m are different. Our estimates of $\Delta\Psi$ (Huang et al., 2007) of -60 to -70 mV at 700 s with OMN present are much lower than without OMN; this is likely due to dissipation of both ΔpH_m and $\Delta\Psi_m$ gradients because H^+ pumping by complex V to support ΔpH_m (and $\Delta\Psi_m$) was blocked. With OMN present, we estimated Nernst potentials of $+13$ and $+6$ mV, respectively, for Ca^{2+} and H^+ (calculated at 700 s). Based on these Nernst potentials the driving forces for both Ca^{2+} and H^+ would remain inward with OMN present, although their Nernst potentials are reversed compared to those in the absence of OMN. With the slow inward driving force for H^+ , unmatched by H^+ pumping at complex V, pH_m approached pH_e and net $[\text{Ca}^{2+}]_m$ became lowered due to CHE_m . Because inhibiting the MCU with Ru360 caused a robust increase in $[\text{Ca}^{2+}]_e$, this indicated the Ca^{2+} effluxed via CHE_m re-enters via the MCU unless this pathway is blocked. Under the unique condition of collapsed $\Delta\Psi_m$ (100 μM DNP) and ΔpH_m gradients, the secondary, slow uptake of mCa^{2+} is absent (Figures 5A,B, black lines) so that the decline in $[\text{Ca}^{2+}]_m$ via CHE_m is fully observed (Figures 6A,B). Thus, a fall in pH_e strongly supports net mCa^{2+} efflux via CHE_m even though the Nernst potentials indicate continued slow mCa^{2+} influx (via MCU), which indeed occurs if there is remaining $\Delta\Psi_m$. This means that net Ca^{2+} efflux due to CHE_m (Figures 1, 2 and Supplementary Figure S.6) can be exposed by blocking the MCU after the initial bolus of CaCl_2 to prevent further mCa^{2+} uptake. CHE_m is predicted by the J_{CHE} equation to favor mCa^{2+} efflux in exchange for mH^+ influx based on matrix and buffer ion concentrations obtained with OMN present (Supplementary Figure S.10). Our prediction assumes that Ca^{2+} is exchanged for 2H^+ with equal affinities for both cations, or a higher affinity for H^+ .

Does Transient, Low Conductance mPTP Also Shuttle Ca^{2+} Across the IMM in These Experiments?

Inducing a partial $\Delta\Psi_m$ depolarization was reported to cause a slow influx of mCa^{2+} through low conductance mPTP opening (Saotome et al., 2005). CsA prevented both an increase in mCa^{2+} and the release of the small molecule calcein during simulated ischemia in cardiomyocytes suggesting that transient mPTP opening during ischemia allowed mCa^{2+} influx (Seidlmayer et al., 2015). In the present study adding CaCl_2 in the presence of DNP or an acidic buffer caused falls in $\Delta\Psi_m$, so could low conductance mPTP opening have contributed to the secondary, slow increase or decrease in $[\text{Ca}^{2+}]_m$ we observed in the absence or presence of OMN? We doubt this for the following reasons: (1) ROS, adenine nucleotide levels, and other factors are believed to contribute to mPTP formation during IR injury. But in our study we did not utilize IR to induce increases in Ca^{2+} and ROS or decreases in pH_m or $\Delta\Psi_m$; (2) Altering just the driving force for protons across the IMM using DNP or external pH to exchange Ca^{2+} ion for H^+ ions is not compatible for a mechanism to cause or prevent formation of mPTP but it is for inducing mCHE activity; (3) Transient mPTP formation is controversial and based largely on the utility of calcein or other small particles to mark mitochondrial release of small molecules with free flowing ions such as Ca^{2+} (Petronilli et al., 1999); (4) CsA-sensitive transient mPTP opening in individual mitochondria of cardiac myocytes is quite rare even with elevated $[\text{Ca}^{2+}]_m$ or exposure to H_2O_2 (Lu et al., 2016); (4) CsA, or its inhibition of the peptidyl prolyl *cis-trans* isomerase activity of cyclophilin D, has known and unknown effects on mitochondrial function that may be unrelated to mPTP formation (Giorgio et al., 2010). Some interpretations on effects of cyclophilin D, via CsA, may pertain to changes in Ca^{2+} flux due to mCHE rather than transitional mPTP opening.

CsA Ceases Activation of CHE_m

CsA unexpectedly stopped the secondary CaCl_2 -induced effects attributed to CHE_m . CsA ceased all apparent CHE_m activity after adding CaCl_2 when pH_e was 6.9 or 7.15, as assessed by measurements of extra-matrix $[\text{Ca}^{2+}]_e$, pH_m , and $\Delta\Psi_m$ (Supplementary Figures S.1A–C). CsA did not blunt the partial $\Delta\Psi_m$ depolarization induced by DNP alone at pH_e 7.15, but did delay full $\Delta\Psi_m$ depolarization induced by adding CaCl_2 after DNP (Supplementary Figures S.7A,B). We do not believe the slow, attenuated decreases in extrusion of Ca^{2+} or slow fall in matrix pH observed in the presence of CsA are directly related to inhibition of permanent or transient mPTP opening. CsA did not directly prevent the $\Delta\Psi_m$ depolarization that occurs during CHE_m or with addition of DNP alone. In the absence of CsA (Figures 1A–C), the observed changes in pH_m , external $[\text{Ca}^{2+}]_e$, and $\Delta\Psi_m$, induced by adding CaCl_2 at extra-matrix pH 6.9, occurred very slowly over 25–30 min; this is indicative of slow cation exchange activity, not mPTP. Moreover, full $\Delta\Psi_m$ depolarization was incomplete. CsA or its inhibition of cyclophilin D may obviate the conditions for matrix H^+ influx or mCa^{2+} efflux as well as Ca^{2+} recycling via the MCU. CsA

may prevent dissipation of the ΔpH gradient when the external pH is low. Since the results obtained in the presence of CsA are not compatible with preventing or delaying mPTP opening, the effects of CsA in this setting are unclear. Additional experiments will be needed to delineate the mechanism of CsA on preventing CHE_m .

Other Potential Limitations of the Study

One important limitation of our study is the lack of a selective inhibitor of CHE_m to aid in defining a more precise mechanism of action. Since the gene code for LETM1 and its protein sequence are known, point mutations (Tsai et al., 2014) and knockdowns (Jiang et al., 2013; Doonan et al., 2014) in mammalian models will be helpful to assess mechanisms and kinetics of this cation antiporter; but it remains unclear if LETM1 mediates CHE_m exclusively, or at all. Another limitation is that mitochondria were examined outside their normal milieu so that the contributions of ATP synthesis by glycolysis and ATP hydrolysis for cellular metabolic support could not be assessed. Experiments were conducted at room temperature at which metabolism would be lower and buffering capacity different than at 37°C . The activity of CHE_m during cardiac IR is unknown and mCa^{2+} efflux in cardiac mitochondria may occur primarily via the NCE_m and not CHE_m . Nevertheless, induction of CHE_m could occur *in vivo* during IR injury under very specific circumstances of trans-IMM cationic imbalance. Evaluation of CHE_m activity in cardiac myocytes after IR injury should be helpful to design protective strategies using this mechanism.

CONCLUSION

This study furnishes new insights into the bioenergetic and dynamic mechanisms in cardiac cell mitochondria of delayed, slow mCa^{2+} influx via the MCU, and mCa^{2+} efflux via the pH_m -dependent CHE_m . We demonstrate the kinetics of slow changes in mCa^{2+} loading/unloading that are linked to unblocked vs. blocked ATP_m hydrolysis to decrease vs. increase pH_m , respectively, after partial depolarization by DNP. We found that after an initial CaCl_2 bolus there is slow mCa^{2+} influx (Ca^{2+} leak) through a Ru360-sensitive pathway if H^+ pumping counteracts a H^+ leak; however, there is net slow mCa^{2+} efflux that overrides $\Delta\Psi_m$ -mediated Ca^{2+} influx that is activated via CHE_m if there is a high ΔpH_m gradient. In cardiac mitochondria, the rapid and slow mode of uptake of mCa^{2+} appears to be dependent primarily on the trans-membrane $[\text{Ca}^{2+}]$ and $\Delta\Psi_m$ gradients if outward H^+ pumping counteracts inward H^+ entry. In contrast, slow extrusion of mCa^{2+} by CHE_m appears to be dependent primarily on the $[\Delta\text{H}^+]_m$ gradient induced by H^+ influx/leak by DNP or by an acidic pH_e . Importantly, if NCE_m

REFERENCES

Aldakkak, M., Stowe, D. F., Cheng, Q., Kwok, W. M., and Camara, A. K. (2010). Mitochondrial matrix K^+ flux independent of large-conductance Ca^{2+} -activated K^+ channel opening. *Am. J. Physiol. Cell Physiol.* 298, C530–C541. doi: 10.1152/ajpcell.00468.2009

and NHE_m are inactivated, blocking complex V might prevent delayed Ca^{2+} overload and instead stimulate Ca^{2+} extrusion via CHE_m if there is an inward H^+ leak. In intact cells, this can also serve to preserve TCA cycle-generated ATP, i.e., substrate level phosphorylation. Such passive homeostatic balance of $\Delta[\text{Ca}^{2+}]_m$ may occur during cardiac injury when there is mCa^{2+} loading accompanied by declines in NADH redox state, pH_m and Ψ_m . We conclude that the differences in the rate and magnitude of mCa^{2+} influx/efflux in partially depolarized mitochondria, in the presence or absence of F_0F_1 -ATPase activity, can be ascribed to the underlying changes in *pmf* components, ΔpH_m and $\Delta\Psi_m$, after rapid mCa^{2+} loading.

AUTHOR CONTRIBUTIONS

DS proposed the study and its initial design. JH conducted most experiments, carried out initial statistical analysis, constructed initial figures, and participated in design, interpretation and writing. AG, AB, CB, CN, and MB conducted supporting experiments. AC, W-MK, and RD participated in theoretical interpretation of the results and text editing. DS and AC supervised the team in subsequent experimental designs, interpretation of results, and manuscript construction and writing.

FUNDING

This project was supported by grants from the National Institutes of Health (R01HL089514, R01HL095122 and 5T35HL072483) and the Veterans Administration (Merit Review BX820405P and BX002539).

ACKNOWLEDGMENTS

The authors wish to thank Drs. Mohammed Aldakkak, Jason Bazil, Shivendra G. Tewari, Venkat Pannala, Kalyan C. Vinnakota, and Gayathri Natarajan for their help and advice, laboratory manager James S. Heisner for technical assistance and supporting experiments, and medical student David S. Lambert for discussions on follow up studies.

SUPPLEMENTARY MATERIAL

The Supplementary Material for this article can be found online at: <https://www.frontiersin.org/articles/10.3389/fphys.2018.01914/full#supplementary-material>

Austin, S., Tavakoli, M., Pfeiffer, C., Seifert, J., Mattarei, A., De Stefani, D., et al. (2017). LETM1-mediated K^+ and Na^+ homeostasis regulates mitochondrial Ca^{2+} efflux. *Front. Physiol.* 8:839. doi: 10.3389/fphys.2017.00839

Azzone, G. F., Pozzan, T., Massari, S., Bragadin, M., and Dell'Antone, P. (1977). H^+ /site ratio and steady state distribution of divalent cations in mitochondria. *FEBS Lett.* 78, 21–24. doi: 10.1016/0014-5793(77)80264-0

- Bains, R., Moe, M. C., Larsen, G. A., Berg-Johnsen, J., and Vinje, M. L. (2006). Volatile anaesthetics depolarize neural mitochondria by inhibition of the electron transport chain. *Acta Anaesthesiol. Scand.* 50, 572–579. doi: 10.1111/j.1399-6576.2006.00988.x
- Bazil, J. N., Blomeyer, C. A., Pradhan, R. K., Camara, A. K., and Dash, R. K. (2013). Modeling the calcium sequestration system in isolated guinea pig cardiac mitochondria. *J. Bioenerg. Biomembr.* 45, 177–188. doi: 10.1007/s10863-012-9488-2
- Bernardi, P. (1999). Mitochondrial transport of cations: channels, exchangers, and permeability transition. *Physiol. Rev.* 79, 1127–1155. doi: 10.1152/physrev.1999.79.4.1127
- Bernardi, P., Paradisi, V., Pozzan, T., and Azzzone, G. F. (1984). Pathway for uncoupler-induced calcium efflux in rat liver mitochondria: inhibition by ruthenium red. *Biochemistry* 23, 1645–1651. doi: 10.1021/bi00303a010
- Blomeyer, C. A., Bazil, J. N., Stowe, D. F., Pradhan, R. K., Dash, R. K., and Camara, A. K. (2013). Dynamic buffering of mitochondrial Ca²⁺ during Ca²⁺ uptake and Na⁺-induced Ca²⁺ release. *J. Bioenerg. Biomembr.* 45, 189–202. doi: 10.1007/s10863-012-9483-7
- Boelens, A. D., Pradhan, R. K., Blomeyer, C. A., Camara, A. K., Dash, R. K., and Stowe, D. F. (2013). Extra-matrix Mg²⁺ limits Ca²⁺ uptake and modulates Ca²⁺ uptake-independent respiration and redox state in cardiac isolated mitochondria. *J. Bioenerg. Biomembr.* 45, 203–218. doi: 10.1007/s10863-013-9500-5
- Boyman, L., Williams, G. S., Khananshvil, D., Sekler, I., and Lederer, W. J. (2013). NCLX: the mitochondrial sodium calcium exchanger. *J. Mol. Cell Cardiol.* 59, 205–213. doi: 10.1016/j.yjmcc.2013.03.012
- Brand, M. D. (1985). Electroneutral efflux of Ca²⁺ from liver mitochondria. *Biochem. J.* 225, 413–419. doi: 10.1042/bj2250413
- Brand, M. D., and Nicholls, D. G. (2011). Assessing mitochondrial dysfunction in cells. *Biochem. J.* 435, 297–312. doi: 10.1042/BJ20110162
- Brandes, R., and Bers, D. M. (1997). Intracellular Ca²⁺ increases the mitochondrial NADH concentration during elevated work in intact cardiac muscle. *Circ. Res.* 80, 82–87. doi: 10.1161/01.RES.80.1.82
- Brookes, P. S., Yoon, Y., Robotham, J. L., Anders, M. W., and Sheu, S. S. (2004). Calcium, ATP, and ROS: a mitochondrial love-hate triangle. *Am. J. Physiol. Cell Physiol.* 287, C817–C833. doi: 10.1152/ajpcell.00139.2004
- Camara, A. K., Lesnfsky, E. J., and Stowe, D. F. (2010). Potential therapeutic benefits of strategies directed to mitochondria. *Antioxid. Redox. Signal.* 13, 279–347. doi: 10.1089/ars.2009.2788
- Chinopoulos, C. (2011). Mitochondrial consumption of cytosolic ATP: not so fast. *FEBS Lett* 585, 1255–1259. doi: 10.1016/j.febslet.2011.04.004
- Chinopoulos, C., and Adam-Vizi, V. (2010). Mitochondria as ATP consumers in cellular pathology. *Biochim. Biophys. Acta* 1802, 221–227. doi: 10.1016/j.bbabis.2009.08.008
- Chinopoulos, C., Gerencser, A. A., Mandi, M., Mathe, K., Torocsik, B., Doczi, J., et al. (2010). Forward operation of adenine nucleotide translocase during F0F1-ATPase reversal: critical role of matrix substrate-level phosphorylation. *FASEB J.* 24, 2405–2416. doi: 10.1096/fj.09-149898
- Cross, R. L., and Muller, V. (2004). The evolution of A-, F-, and V-type ATP synthases and ATPases: reversals in function and changes in the H⁺/ATP coupling ratio. *FEBS Lett.* 576, 1–4. doi: 10.1016/j.febslet.2004.08.065
- Csordas, G., Varnai, P., Golenar, T., Roy, S., Purkins, G., Schneider, T. G., et al. (2010). Imaging interorganelle contacts and local calcium dynamics at the ER-mitochondrial interface. *Mol. Cell.* 39, 121–132. doi: 10.1016/j.molcel.2010.06.029
- Dash, R. K., and Beard, D. A. (2008). Analysis of cardiac mitochondrial Na⁺-Ca²⁺ exchanger kinetics with a biophysical model of mitochondrial Ca²⁺ handling suggests a 3:1 stoichiometry. *J. Physiol.* 586, 3267–3285. doi: 10.1113/jphysiol.2008.151977
- Dash, R. K., Qi, F., and Beard, D. A. (2009). A biophysically based mathematical model for the kinetics of mitochondrial calcium uniporter. *Biophys. J.* 96, 1318–1332. doi: 10.1016/j.bpj.2008.11.005
- De Marchi, U., Santo-Domingo, J., Castelbou, C., Sekler, I., Wiederkehr, A., and Demaurex, N. (2014). NCLX protein, but not LETM1, mediates mitochondrial Ca²⁺ extrusion, thereby limiting Ca²⁺-induced NAD(P)H production and modulating matrix redox state. *J. Biol. Chem.* 289, 20377–20385. doi: 10.1074/jbc.M113.540898
- De Stefani, D., Patron, M., and Rizzuto, R. (2015). Structure and function of the mitochondrial calcium uniporter complex. *Biochim. Biophys. Acta* 1853, 2006–2011. doi: 10.1016/j.bbamcr.2015.04.008
- Delcamp, T. J., Dales, C., Ralenkotter, L., Cole, P. S., and Hadley, R. W. (1998). Intramitochondrial [Ca²⁺] and membrane potential in ventricular myocytes exposed to anoxia-reoxygenation. *Am. J. Physiol.* 275(2 Pt 2), H484–H494. doi: 10.1152/ajpheart.1998.275.2.H484
- Demaurex, N., Poburko, D., and Frieden, M. (2009). Regulation of plasma membrane calcium fluxes by mitochondria. *Biochim. Biophys. Acta* 1787, 1383–1394. doi: 10.1016/j.bbabi.2008.12.012
- Denton, R. M., McCormack, J. G., and Edgell, N. J. (1980). Role of calcium ions in the regulation of intramitochondrial metabolism. Effects of Na⁺, Mg²⁺ and ruthenium red on the Ca²⁺-stimulated oxidation of oxoglutarate and on pyruvate dehydrogenase activity in intact rat heart mitochondria. *Biochem. J.* 190, 107–117. doi: 10.1042/bj1900107
- Di Lisa, F., and Bernardi, P. (1998). Mitochondrial function as a determinant of recovery or death in cell response to injury. *Mol. Cell. Biochem.* 184, 379–391. doi: 10.1023/A:1006810523586
- Doonan, P. J., Chandramoorthy, H. C., Hoffman, N. E., Zhang, X., Cardenas, C., Shanmughapriya, S., et al. (2014). LETM1-dependent mitochondrial Ca²⁺ flux modulates cellular bioenergetics and proliferation. *FASEB J.* 28, 4936–4949. doi: 10.1096/fj.14-256453
- Dzdek, J., and Korzeniewski, B. (2008). Control over the contribution of the mitochondrial membrane potential ($\Delta\Psi$) and proton gradient (ΔpH) to the protonmotive force (Δp). In silico studies. *J. Biol. Chem.* 283, 33232–33239. doi: 10.1074/jbc.M802404200
- Froschauer, E., Nowikovsky, K., and Schweyen, R. J. (2005). Electroneutral K⁺/H⁺ exchange in mitochondrial membrane vesicles involves Yol027/LETM1 proteins. *Biochim. Biophys. Acta* 1711, 41–48. doi: 10.1016/j.bbamem.2005.02.018
- Gambassi, G., Hansford, R. G., Sollott, S. J., Hogue, B. A., Lakatta, E. G., and Capogrossi, M. C. (1993). Effects of acidosis on resting cytosolic and mitochondrial Ca²⁺ in mammalian myocardium. *J. Gen. Physiol.* 102, 575–597. doi: 10.1085/jgp.102.3.575
- Giorgio, V., Soriano, M. E., Basso, E., Bisetto, E., Lippe, G., Forte, M. A., et al. (2010). Cyclophilin D in mitochondrial pathophysiology. *Biochim. Biophys. Acta* 1797, 1113–1118. doi: 10.1016/j.bbabi.2009.12.006
- Grover, G. J., Atwal, K. S., Sleph, P. G., Wang, F. L., Monshizadegan, H., Monticello, T., et al. (2004). Excessive ATP hydrolysis in ischemic myocardium by mitochondrial F1F0-ATPase: effect of selective pharmacological inhibition of mitochondrial ATPase hydrolase activity. *Am. J. Physiol. Heart Circ. Physiol.* 287, H1747–H1755. doi: 10.1152/ajpheart.01019.2003
- Gunter, K. K., Zuscik, M. J., and Gunter, T. E. (1991). The Na⁺-independent Ca²⁺ efflux mechanism of liver mitochondria is not a passive Ca²⁺/2H⁺ exchanger. *J. Biol. Chem.* 266, 21640–21648.
- Gunter, T. E., Gunter, K. K., Sheu, S. S., and Gavin, C. E. (1994). Mitochondrial calcium transport: physiological and pathological relevance. *Am. J. Physiol.* 267(2 Pt 1), C313–C339. doi: 10.1152/ajpcell.1994.267.2.C313
- Gunter, T. E., and Pfeiffer, D. R. (1990). Mechanisms by which mitochondria transport calcium. *Am. J. Physiol.* 258(5 Pt 1), C755–C786. doi: 10.1152/ajpcell.1990.258.5.C755
- Gursahani, H. I., and Schaefer, S. (2004). Acidification reduces mitochondrial calcium uptake in rat cardiac mitochondria. *Am. J. Physiol. Heart Circ. Physiol.* 287, H2659–H2665. doi: 10.1152/ajpheart.00344.2004
- Haumann, J., Dash, R. K., Stowe, D. F., Boelens, A., Beard, D. A., and Camara, A. K. S. (2010). Mitochondrial free [Ca²⁺] increases during ATP/ADP antiport and ADP phosphorylation: exploration of mechanisms. *Biophys. J.* 99, 997–1006. doi: 10.1016/j.bpj.2010.04.069
- Heinen, A., Camara, A. K., Aldakkak, M., Rhodes, S. S., Riess, M. L., and Stowe, D. F. (2007). Mitochondrial Ca²⁺-induced K⁺ influx increases respiration and enhances ROS production while maintaining membrane potential. *Am. J. Physiol. Cell Physiol.* 292, C148–C156. doi: 10.1152/ajpcell.00215.2006
- Hoppe, U. C. (2010). Mitochondrial calcium channels. *FEBS Lett.* 584, 1975–1981. doi: 10.1016/j.febslet.2010.04.017

- Huang, M., Camara, A. K., Stowe, D. F., Qi, F., and Beard, D. A. (2007). Mitochondrial inner membrane electrophysiology assessed by rhodamine-123 transport and fluorescence. *Ann. Biomed. Eng.* 35, 1276–1285. doi: 10.1007/s10439-007-9265-2
- Jennings, R. B., Reimer, K. A., and Steenbergen, C. (1991). Effect of inhibition of the mitochondrial ATPase on net myocardial ATP in total ischemia. *J. Mol. Cell Cardiol.* 23, 1383–1395. doi: 10.1016/0022-2828(91)90185-0
- Jiang, D., Zhao, L., and Clapham, D. E. (2009). Genome-wide RNAi screen identifies LETM1 as a mitochondrial Ca²⁺/H⁺ antiporter. *Science* 326, 144–147. doi: 10.1126/science.1175145
- Jiang, D., Zhao, L., Clish, C. B., and Clapham, D. E. (2013). LETM1, the mitochondrial Ca²⁺/H⁺ antiporter, is essential for normal glucose metabolism and alters brain function in Wolf-Hirschhorn syndrome. *Proc. Natl. Acad. Sci. U.S.A.* 110, E2249–E2254. doi: 10.1073/pnas.1308558110
- Leysens, A., Nowicky, A. V., Patterson, L., Crompton, M., and Duchon, M. R. (1996). The relationship between mitochondrial state, ATP hydrolysis, [Mg²⁺]_i and [Ca²⁺]_i studied in isolated rat cardiomyocytes. *J. Physiol.* 496, 111–128. doi: 10.1113/jphysiol.1996.sp021669
- Lu, X., Kwong, J. Q., Molkentin, J. D., and Bers, D. M. (2016). Individual cardiac mitochondria undergo rare transient permeability transition pore openings. *Circ. Res.* 118, 834–841. doi: 10.1161/CIRCRESAHA.115.308093
- Malli, R., and Graier, W. F. (2010). Mitochondrial Ca²⁺ channels: great unknowns with important functions. *FEBS Lett.* 584, 1942–1947. doi: 10.1016/j.febslet.2010.01.010
- McCormack, J. G., and Denton, R. M. (1980). Role of calcium ions in the regulation of intramitochondrial metabolism. Properties of the Ca²⁺-sensitive dehydrogenases within intact uncoupled mitochondria from the white and brown adipose tissue of the rat. *Biochem. J.* 190, 95–105. doi: 10.1042/bj1900095
- Metelkin, E., Demin, O., Kovacs, Z., and Chinopoulos, C. (2009). Modeling of ATP-ADP steady-state exchange rate mediated by the adenine nucleotide translocase in isolated mitochondria. *FEBS J.* 276, 6942–6955. doi: 10.1111/j.1742-4658.2009.07394.x
- Murphy, E., and Steenbergen, C. (2008). Mechanisms underlying acute protection from cardiac ischemia-reperfusion injury. *Physiol. Rev.* 88, 581–609. doi: 10.1152/physrev.00024.2007
- Nishizawa, T., Kita, S., Maturana, A. D., Furuya, N., Hirata, K., Kasuya, G., et al. (2013). Structural basis for the counter-transport mechanism of a H⁺/Ca²⁺ exchanger. *Science* 341, 168–172. doi: 10.1126/science.1239002
- Nowikovsky, K., Froschauer, E. M., Zsurka, G., Samaj, J., Reipert, S., Kolisek, M., et al. (2004). The LETM1/YOL027 gene family encodes a factor of the mitochondrial K⁺ homeostasis with a potential role in the Wolf-Hirschhorn syndrome. *J. Biol. Chem.* 279, 30307–30315. doi: 10.1074/jbc.M403607200
- Nowikovsky, K., Pozzan, T., Rizzuto, R., Scorrano, L., and Bernardi, P. (2012). Perspectives on: SGP symposium on mitochondrial physiology and medicine: the pathophysiology of LETM1. *J. Gen. Physiol.* 139, 445–454. doi: 10.1085/jgp.201110757
- O'Rourke, B., Cortassa, S., and Aon, M. A. (2005). Mitochondrial ion channels: gatekeepers of life and death. *Physiology* 20, 303–315. doi: 10.1152/physiol.00020.2005
- O-Uchi, J., Jhun, B. S., Hurst, S., Bisetto, S., Gross, P., Chen, M., et al. (2013). Overexpression of ryanodine receptor type 1 enhances mitochondrial fragmentation and Ca²⁺-induced ATP production in cardiac H9c2 myoblasts. *Am. J. Physiol. Heart Circ. Physiol.* 305, H1736–H1751. doi: 10.1152/ajpheart.00094.2013
- Petronilli, V., Miotto, G., Canton, M., Brini, M., Colonna, R., Bernardi, P., et al. (1999). Transient and long-lasting openings of the mitochondrial permeability transition pore can be monitored directly in intact cells by changes in mitochondrial calcein fluorescence. *Biophys. J.* 76, 725–734. doi: 10.1016/S0006-3495(99)77239-5
- Pozzan, T., Bragadin, M., and Azzone, G. F. (1977). Disequilibrium between steady-state Ca²⁺ accumulation ratio and membrane potential in mitochondria. Pathway and role of Ca²⁺ efflux. *Biochemistry* 16, 5618–5625. doi: 10.1021/bi00644a036
- Riess, M. L., Camara, A. K., Heinen, A., Eells, J. T., Henry, M. M., and Stowe, D. F. (2008). K_{ATP} channel openers have opposite effects on mitochondrial respiration under different energetic conditions. *J. Cardiovasc. Pharmacol.* 51, 483–491. doi: 10.1097/FJC.0b013e31816bf4a4
- Riess, M. L., Camara, A. K., Novalija, E., Chen, Q., Rhodes, S. S., and Stowe, D. F. (2002). Anesthetic preconditioning attenuates mitochondrial Ca²⁺ overload during ischemia in Guinea pig intact hearts: reversal by 5-hydroxydecanoic acid. *Anesth. Analg.* 95, 1540–1546. doi: 10.1097/0000539-200212000-00013
- Rottenberg, H., and Marbach, M. (1990). The Na⁺-independent Ca²⁺ efflux system in mitochondria is a Ca²⁺/2H⁺ exchange system. *FEBS Lett.* 274, 65–68. doi: 10.1016/0014-5793(90)81330-Q
- Ryu, S. Y., Beutner, G., Kinnally, K. W., Dirksen, R. T., and Sheu, S. S. (2011). Single channel characterization of the mitochondrial ryanodine receptor in heart mitoplasts. *J. Biol. Chem.* 286, 21324–21329. doi: 10.1074/jbc.C111.245597
- Saotome, M., Katoh, H., Satoh, H., Nagasaka, S., Yoshihara, S., Terada, H., et al. (2005). Mitochondrial membrane potential modulates regulation of mitochondrial Ca²⁺ in rat ventricular myocytes. *Am. J. Physiol. Heart Circ. Physiol.* 288, H1820–H1828. doi: 10.1152/ajpheart.00589.2004
- Seidlmayer, L. K., Juettner, V. V., Kettlewell, S., Pavlov, E. V., Blatter, L. A., and Dedkova, E. N. (2015). Distinct mPTP activation mechanisms in ischaemia-reperfusion: contributions of Ca²⁺, ROS, pH, and inorganic polyphosphate. *Cardiovasc. Res.* 106, 237–248. doi: 10.1093/cvr/cvv097
- Shao, J., Fu, Z., Ji, Y., Guan, X., Guo, S., Ding, Z., et al. (2016). Leucine zipper-EF-hand containing transmembrane protein 1 (LETM1) forms a Ca²⁺/H⁺ antiporter. *Sci. Rep.* 6:34174. doi: 10.1038/srep34174
- Stowe, D. F., and Camara, A. K. (2009). Mitochondrial reactive oxygen species production in excitable cells: modulators of mitochondrial and cell function. *Antioxid. Redox. Signal.* 11, 1373–1414. doi: 10.1089/ARS.2008.2331
- Tewari, S. G., Camara, A. K., Stowe, D. F., and Dash, R. K. (2014). Computational analysis of Ca²⁺ dynamics in isolated cardiac mitochondria predicts two distinct modes of Ca²⁺ uptake. *J. Physiol.* 592(Pt 9), 1917–1930. doi: 10.1113/jphysiol.2013.268847
- Tsai, M. F., Jiang, D., Zhao, L., Clapham, D., and Miller, C. (2014). Functional reconstitution of the mitochondrial Ca²⁺/H⁺ antiporter LETM1. *J. Gen. Physiol.* 143, 67–73. doi: 10.1085/jgp.201311096
- Valdez, L. B., Zaobornyj, T., and Boveris, A. (2006). Mitochondrial metabolic states and membrane potential modulate mtNOS activity. *Biochim. Biophys. Acta* 1757, 166–172. doi: 10.1016/j.bbabi.2006.02.013
- Wan, B., LaNoue, K. F., Cheung, J. Y., and Scaduto, R. C. Jr. (1989). Regulation of citric acid cycle by calcium. *J. Biol. Chem.* 264, 13430–13439.
- Wingrove, D. E., Amatruda, J. M., and Gunter, T. E. (1984). Glucagon effects on the membrane potential and calcium uptake rate of rat liver mitochondria. *J. Biol. Chem.* 259, 9390–9394.

Conflict of Interest Statement: The authors declare that the research was conducted in the absence of any commercial or financial relationships that could be construed as a potential conflict of interest.

Citation: Haumann J, Camara AKS, Gadicherla AK, Navarro CD, Boelens AD, Blomeyer CA, Dash RK, Boswell MR, Kwok W-M and Stowe DF (2019) Slow Ca²⁺ Efflux by Ca²⁺/H⁺ Exchange in Cardiac Mitochondria Is Modulated by Ca²⁺ Re-uptake via MCU, Extra-Mitochondrial pH, and H⁺ Pumping by F₀F₁-ATPase. *Front. Physiol.* 9:1914. doi: 10.3389/fphys.2018.01914

Copyright © 2019 Haumann, Camara, Gadicherla, Navarro, Boelens, Blomeyer, Dash, Boswell, Kwok and Stowe. This is an open-access article distributed under the terms of the Creative Commons Attribution License (CC BY). The use, distribution or reproduction in other forums is permitted, provided the original author(s) and the copyright owner(s) are credited and that the original publication in this journal is cited, in accordance with accepted academic practice. No use, distribution or reproduction is permitted which does not comply with these terms.